DIFFERENTIAL GPS: CONCEPTS AND QUALITY CONTROL

prof.dr.ir. P.J.G. Teunissen
Delft Geodetic Computing Centre (LGR)
Department of Geodesy
Delft University of Technology
Thijsseweg 11, 2629 JA Delft
The Netherlands

INVITED LECTURE
for the
Netherlands Institute of Navigation (NIN)
Amsterdam, September 27 1991

Delft Geodetic Computing Centre (LGR)
Thijsseweg 11, 2629 JA DELFT, The Netherlands

C O N T E N T S

1. INTRODUCTION

The satellite-based Global Positioning System (GPS) is rapidly becoming the major positioning system for a variety of geodetic applications. With the completion of the satellite constellation in the early 1990s, the system will provide 24-hour all-weather precise positioning capabilities that extend to virtually all parts of the globe.

Positioning with GPS can be divided into single-receiver single point positioning and multi-receiver positioning relative to a simultaneously observing reference receiver. Although the GPS system has originally been designed for single point positioning to support military navigation needs,

L A N D	S E A	A I R
o Geodynamics (plate tectonics, sealevel rise; 0.01 - 0.1 ppm over intercontinental distances)	o Hydrographic surveying (0.1 - 10 m)	o Aero-triangulation (depending on mapping scale: submetre to several meters)
o Continental 3D reference frame (0.1 - 1 ppm)	o Marine 3D seismic surveys (1 - 5 m)	o Airborne laserprofiling (hor.: 1 - 10 m, vert.: 0.5 - 1 m)
o National hor. and vert. control networks (1 - 10 ppm)	o Marine gravity surveys (< 10 cm/s for Eötvös correction < 1 mgal)	o Airborne gravimetry (hor.: 50 m, vert.: 2 m, vel.: 10 cm/s)
o Surface and platform subsidence monitoring (1 ppm)	o Navigation in coastal area (50 - 100 m)	o Airborne laser bathymetry (hor.: 15 m)
o Large scale topography (10 - 100 ppm)	o Navigation in open waters (1 - several km)	o Airtransport terminal approach (hor.: 0.1 - 0.5 km)
o Land navigation (10 - 50 m)		o Airtransport terminal area (hor.: 0.5 - 1 km)
		o Airtransport en route (1 - several km)

Table 1: GPS positioning applications with precision requirements (1σ)

the most precise results are obtained in relative mode. This is because relative positioning enables one to eliminate or greatly reduce errors that are common to the simultaneously observing receivers. Some typical positioning applications for which GPS already has been used or may be used in the near future, are given in table 1 together with their precision requirements.

This paper reviews the elementary principles of differential or relative positioning with GPS. It discusses various methods of relative GPS positioning and their precision requirements, considers static and kinematic applications, and emphasizes the increasing conformance in real-time and post-processing GPS positioning techniques. The paper is organized as follows. In chapter 2 we introduce the two basic GPS observables, namely the pseudo range observable and the carrier phase observable. Chapter 3 is devoted to the different concepts of relative GPS positioning. In this chapter a distinction is made between four concepts of relative positioning with GPS. The first two (static and semi-kinematic surveying) are network oriented, whereas the last two (kinematic surveying and DGPS navigation) are trajectory oriented. The conformances of and differences between the four concepts are discussed. Finally chapter 4 provides for an introduction in quality control. Using the simplest possible model for GPS positioning, it is shown how the quality control theory as developed at the Delft Geodetic Computing Centre (LGR) can be applied in order to validate the quality of GPS measurements.

2. GPS OBSERVABLES AND SINGLE POINT POSITIONING

2.1. The pseudo range observable

There are two important types of GPS observables: pseudo ranges and carrier phases (figure 1). The pseudo range is a measure of the distance between the satellite and the receiver at the epochs of transmission and reception of the GPS signals. It is based on measuring the travel time τ_i^j of the satellite signal from satellite j to receiver i (the superscript refers to the satellite and the subscript to the receiver on the earth). The travel time is obtained by correlating identical codes generated by the satellite and by the receiver. The codes generated at the receiver are derived from the receiver's own clock, and the codes of the satellite transmissions are generated by the satellite system of clocks. If we ignore atmospheric propagation effects and any timing errors, then the pseudo range $p_i^j = c\tau_i^j$, with c the speed of light, is just the distance $\|\mathbf{r}^j-\mathbf{r}_i\|$ between satellite j and receiver i, with $\mathbf{r}^j$ and $\mathbf{r}_i$ the position vectors of satellite j and receiver i respectively. Atmospheric propagation delays are however present in the GPS signals. There are two main regions of the atmosphere that need to be considered: the nondispersive troposphere (0-50 km), and the frequency-dispersive ionosphere (100-1000 km). Both regions affect the GPS signals through changes in velocity, and by ray bending. The (metric) delays due to troposphere and ionosphere will be denoted as T_i^j and I_i^j respectively.

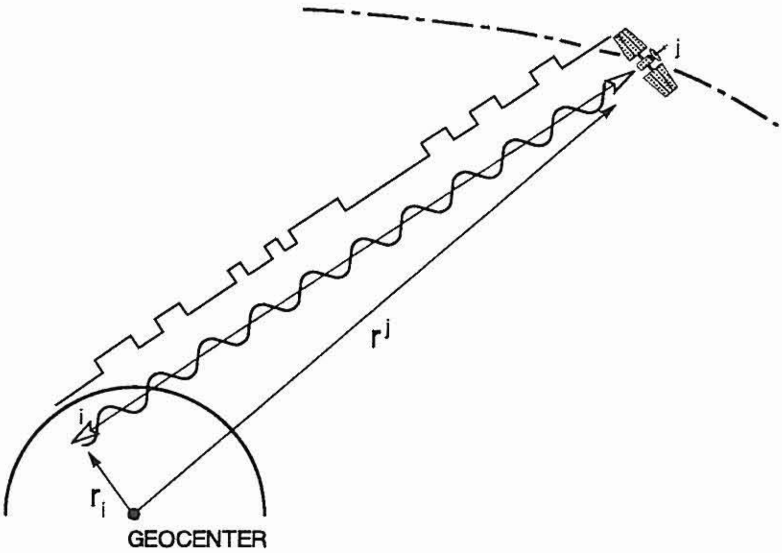

Figure 1: The pseudo range and carrier phase observable

In addition to the atmospheric delays, also errors in receiver (δt_i) and satellite (δt^j) clocks are present in p_i^j, which for this reason is referred to as pseudo range. Therefore,

(1) $$p_i^j = \|\mathbf{r}^j-\mathbf{r}_i\| + c(\delta t_i - \delta t^j) + T_i^j + I_i^j \ .$$

This is the basic equation that relates the pseudo range observable p_i^j to the unknown position vector $\mathbf{r}_i$ of the receiver.

2.2. Single point positioning

The nonlinear pseudo range observation equation (1) shows that given the satellite position $\mathbf{r}^j$ at the time of transmission and given models for the satellite clock errors and propagation delays, four simultaneous observed pseudo ranges are necessary and sufficient for the instantaneous determination of both the receiver's position vector $\mathbf{r}_i$ and receiver clock offset δt_i (figure 2). The satellite position is provided by the satellite ephemeris as contained in the navigation message read by the receiver. Also the offsets of the satellite clocks are transmitted to the user as part of the navigation message. And the atmospheric propagation delays can be computed on the basis of tropospheric and ionospheric models.

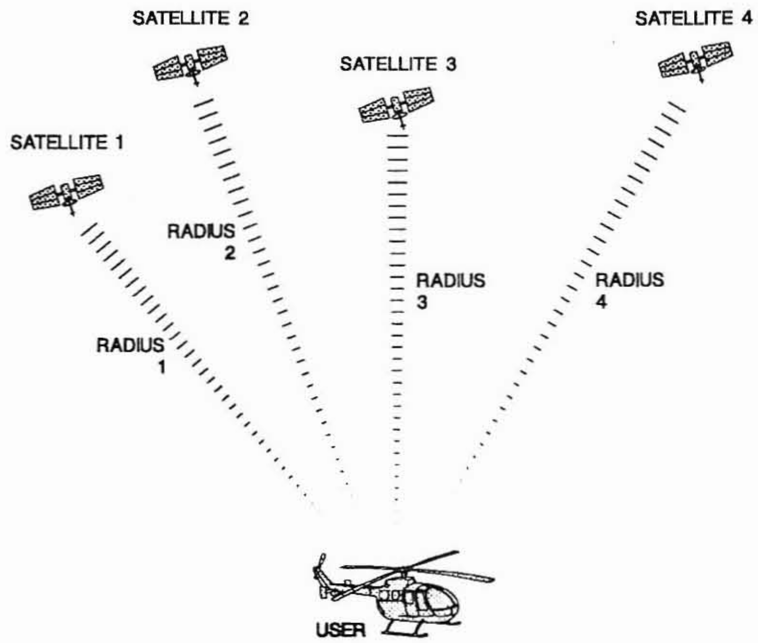

Figure 2: Single point positioning with pseudo ranges

Since four pseudo ranges are minimally needed for instantaneous point positioning, the basic requirement is that there be four satellites visible at any given time anywhere on the earth. This visibility requirement was taken into consideration when designing the basic GPS satellite constellation.
In case more than four pseudo ranges are simultaneously observed, a redundant system of linearized observation equations needs to be solved. This system is usually solved using the principle of least squares. The available redundancy in the data, enables one then to exercise quality control (see chapter 4).

In order to form an error budget for the single point positioning with (C/A-code) pseudo range measurements, the various different error sources first have to be quantified separately:

Receiver measurement noise:
The intrinsic precision of pseudo range measurements is in the order of

1-2 mtr.

Satellite clock:
Satellite clock errors can be predicted to within 10 nanoseconds, which corresponds with 3 mtr.

Satellite ephemeris:
The ability to predict the satellite positions has improved considerably from the early days of GPS. The present capability to predict the satellite ephemeris is such that the range uncertainty lies in the order of 5 mtr or better.

Tropospheric delay compensation:
A GPS signal is bent and slowed in its passage through the troposphere. The tropospheric correction must therefore be subtracted from the observed pseudo range. The propagation delay of the troposphere reaches about 2.0-2.5 mtr at zenith (elevation angle $\varepsilon = 90^{\circ}$) at altitudes near sea level and increases approximately as $1/\sin(\varepsilon)$, yielding about a 20-30 mtr delay at $\varepsilon = 5^{\circ}$ (figure 3).

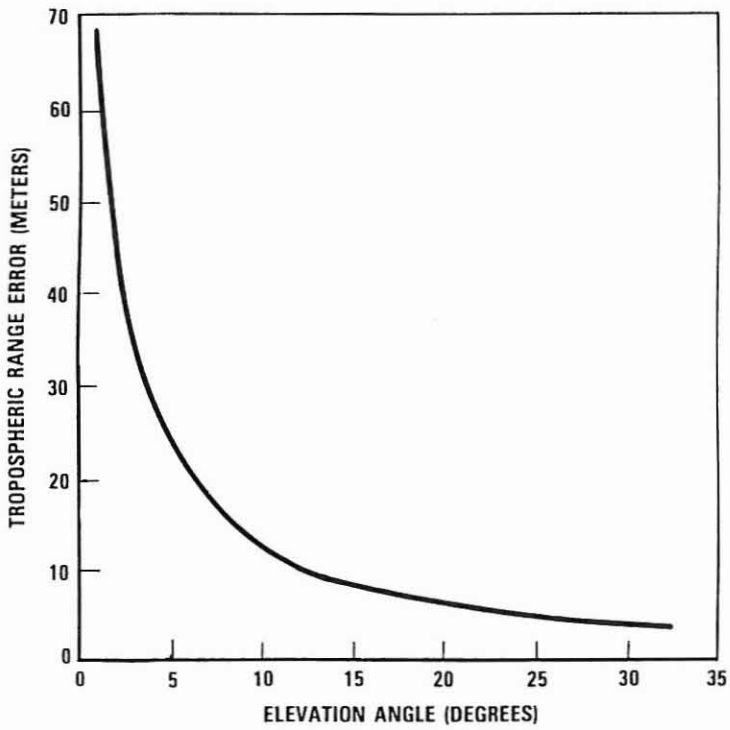

Figure 3: Tropospheric delay as function of elevation angle

The delay depends on the temperature, humidity, and pressure, varies with the height of the receiver, and can vary with the type of terrain below the signal path. There exist various tropospheric refraction models. They can be used together with local measurements of pressure, temperature and humidity, to compute the tropospheric delay correction. If such measurements are not available, standard atmospheric conditions are usually assumed. The models normally used for tropospheric delay correction typically correct for 90 percent of the delay [1]. The remaining range uncertainty after compensation for the tropospheric delay is therefore in the order of 2 mtr.

Ionospheric delay compensation:

The free electrons in the earth's ionosphere interact strongly with any electromagnetic signal in the frequency range of GPS (L_1 = 1575.42 MHz, λ_1 = 19 cm ; L_2 = 1227.60 MHz, λ_2 = 24.4 cm). Ionospheric effects are proportional to the Total Electron Content (TEC) along the signal path and therefore depend on solar activity, receiver location, viewing direction, and time of the day. The ionospheric delay can be as much as 20-30 metres during the day to 2-6 metres at night (figure 4).

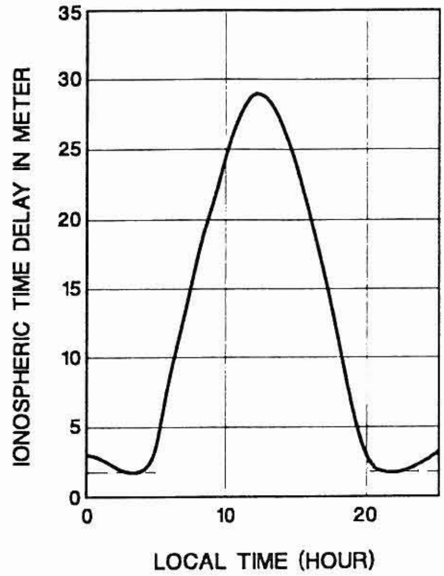

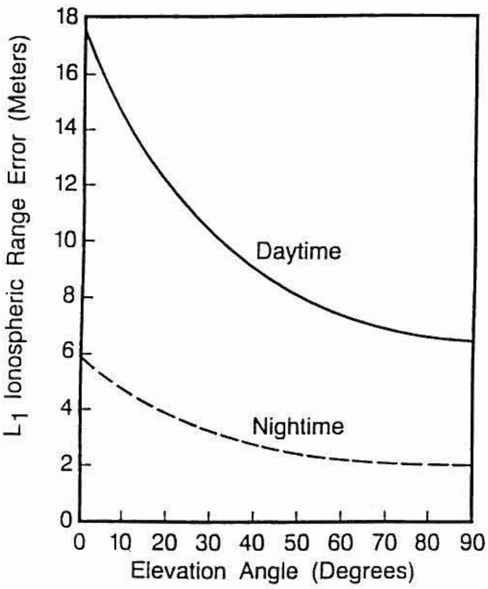

Figure 4: Ionospheric delay as function of time and elevation angle

A first-order expression for the ionospheric time delay in metres is

$$I_i^j = a/f^2, \quad (2)$$

where f denotes the frequency of the signal in Hertz and the factor a reflects the time-variations of the TEC. Since the delay is inversely proportional to the square of the frequency, higher frequencies are less affected by the ionosphere than lower frequencies. This is why the high-frequency GPS signals pass relatively well through the ionosphere. The frequency-dispersive nature of the ionosphere also makes it possible to eliminate the ionospheric effect with dual frequency receivers. Unfortunately however civilian users will probably not have access to the pseudo range measurements on the second L_2 frequency. One therefore has to rely on ionospheric models. These models typically correct for 50 percent of the ionospheric delay [2,3]. The remaining uncertainty after ionospheric compensation is in the order of 5-10 mtr.

Multipath interference:

One speaks of multipath if the received signal is composed of the direct line of sight signal and one or more constituents which have propagated along paths of a different length (figure 5).

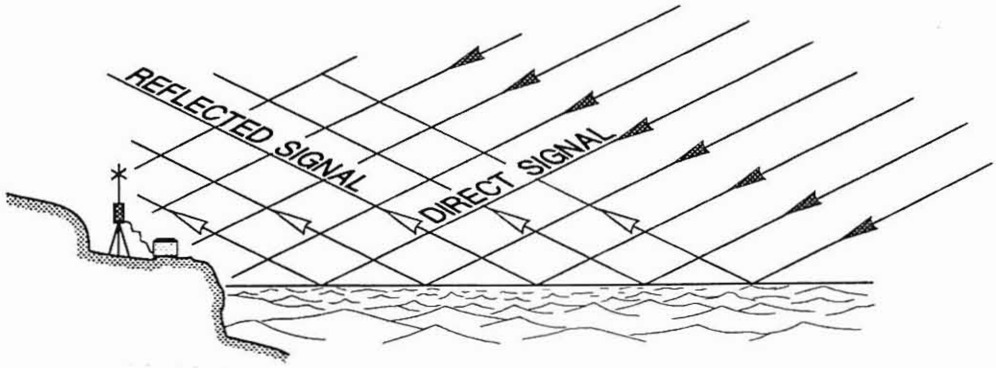

Figure 5: Single horizontal reflector multipath

Since most GPS antennas are omnidirectional, enabling signals from several satellites to be received simultaneously, these antennas are susceptible to multipath because of reflections from nearby objects. Multipath corrupts the pseudo range measurements with systematic, time-dependent sinusoidal signals associated with variable receiver-satellite-reflector geometry over a pass. Low elevation angle observations tend to be most affected, and for this reason a cut-off angle of 10°-20° above the horizon is usually employed. Multipath can be minimized through use of radio frequency absorbent material around the base of the antenna, mounting antennas close to the ground, and careful site selection, choosing sites well away from planar-reflecting surfaces. Without precautions, range errors due to multipath interference can reach values in the order of 2-10 metres, with a required signal averaging time to remove the multipath cyclical effects of 5-60 minutes [4]. In a conditioned environment however, uncertainties due to multipath are generally estimated to be in the order of 1-2 mtr.

Error Source	C/A-Code error 1 sigma (metre)
Receiver measurement noise	1-2
Satellite clock	3
Satellite ephemeris	5
Tropospheric delay compensation	2
Ionospheric delay compensation	5-10
Multipath	1-2
User Equivalent Range Error	8-12 mtr

Table 2: Pseudo range error budget

Based on the above listed error sources, an application of the error propagation law results in a user equivalent range error for pseudo ranges of 8-12 mtr (see table 2). With the fully configured GPS constellation, having an average HDOP of 1.5 this corresponds to a 1-sigma horizontal radial position error in the order of 12-18 mtr (HDOP = $[\mathrm{sqrt}(\sigma_x^2+\sigma_y^2)]/\sigma^2$).
Originally, when the concept of GPS was still in the designing phase, the positioning precision of GPS for unauthorized users was expected to be about 200 mtr (1 sigma) instead of the feasible precision of about 20 mtr. This unexpected situation prompted the U.S. government to review the security consequences of making such position information available to everyone. The result was that a program, now called Selective Availability (SA), was implemented to incorporate in the new generation Block II GPS satellites precision control for unauthorized users. The implementation of SA is now known to be a combination of manipulation of the broadcasted ephemeris data and the introduction of additional clock errors by deliberately degrading the stability of the on-board atomic clocks (frequency dithering). The policy of the U.S. government is that all satellites will have SA enabled as soon as they are declared operational and that SA is normally set so as to have a horizontal radial position precision of 100 mtr (2 sigma). The level of SA may however be changed as U.S. defense conditions dictate. Figure 6 shows a two-dimensional scatterplot of single GPS position fixes based on pseudo range measurements in the presence of SA.

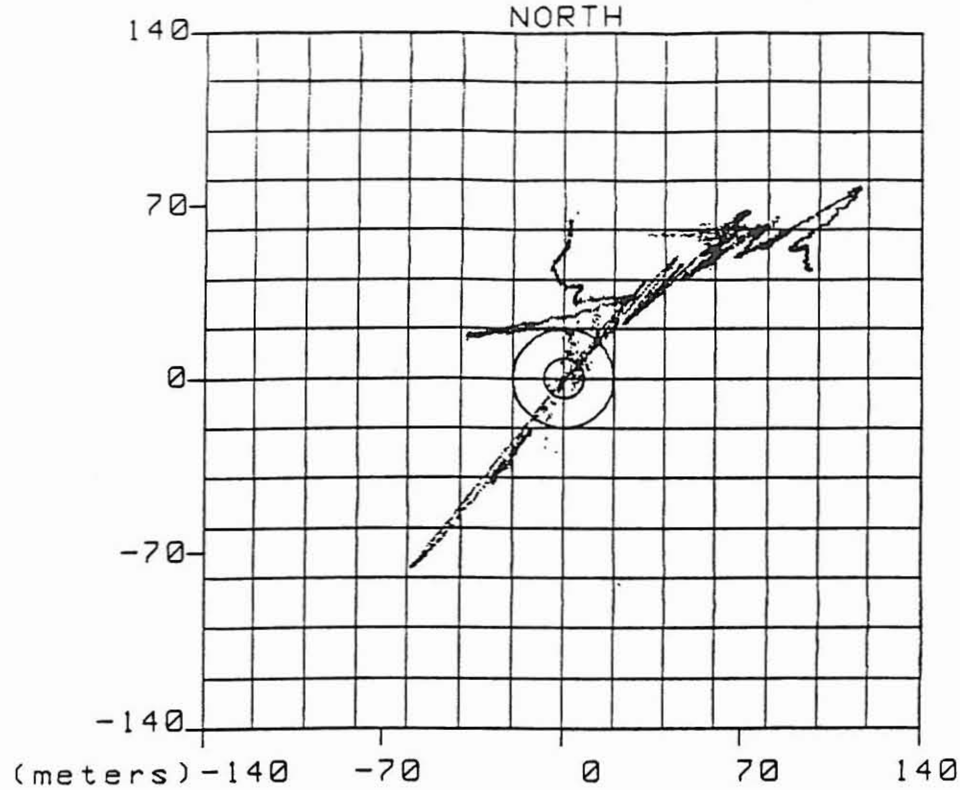

Figure 6: A two-dimensional scatterplot with SA

Although the 100 mtr level is still adequate for many civilian navigation applications such as en route and terminal control requirements, as well as marine oceanic and coastal navigation safety requirements, there are also many navigational applications for which the requirements are not met (see table 1). It therefore became evident that the civilian navigation-community had to devise a set up to allow for an increased precision. Differential GPS-navigation (see section 3.4) provides such a capability.

2.3. The carrier phase observable

It will be clear from the above, that even in the absence of SA, the order of precision for single point positioning based on pseudo ranges, does not meet the requirements of high-precision surveying applications. Fortunately however it is also possible to obtain information on the distance from receiver to satellite through phase measurements on the carrier signal itself. The intrinsic measurement precision of the carrier phase measurements is at the one hundredth of the L_1 19 cm wavelength level. For this reason geodesists and surveyors have been developing since the early days of GPS advanced processing methods for the phase measurements on the carrier itself.

A very brief derivation of the phase observation equation will now be given. The phase of an harmonic is defined as: $\phi = f.t+\Phi$, with frequency f, time t and initial phase Φ. The phase observable ϕ_i^j between receiver i and satellite j is the difference between the phase ϕ^j of the carrier signal of the satellite, measured at the receiver, and the phase ϕ_i of the local oscillator within the receiver at the epoch of measurement. If the frequency of the carrier generated by the local oscillator is constant and identical to the frequency of the carrier as transmitted by the satellite, then: $\phi_i^j = f(t^j-t_i)+\Phi^j-\Phi_i+N_i^j$. The constant N_i^j in this expression denotes the unknown number of integer carrier wavelengths at signal acquisition. If we denote $-(c/f)\phi_i^j$ as P_i^j, and substitute $\|\mathbf{r}^j-\mathbf{r}_i\|$ for $c(t_i-t^j)$, the (metric) phase expression becomes $P_i^j = \|\mathbf{r}^j-\mathbf{r}_i\| + (c/f)(\Phi_i-\Phi^j-N_i^j)$. This expression ignores however propagation effects and is also still based on the assumption of constancy for the satellite and receiver clock frequencies. The complete (metric) phase expression reads therefore,

$$P_i^j = \|\mathbf{r}^j-\mathbf{r}_i\| + c(\delta t_i-\delta t^j) + T_i^j - I_i^j + (c/f)(\Phi_i-\Phi^j-N_i^j) \quad (3)$$

Note the resemblance in structure between the pseudo range observation equation (1) and the (metric) phase observation equation (3). The two equations only differ in the sign of the atmospheric terms and in the term $(c/f)(\Phi_i-\Phi^j-N_i^j)$.

The difference in sign for the atmospheric terms is due to the difference in propagation velocity for the pseudo range code measurements and carrier phase measurements respectively. Since the ionosphere is frequency-dispersive, the group velocity, associated with the pseudo range code measurement, differs from the phase velocity, in the sense that although the effects are equal in magnitude, they are opposite in sign. Thus the group velocity is smaller than in free space, whereas the phase velocity is higher than in free space. This difference in ionospheric delay is referred to as group delay and phase advance. This explains the minus sign of I_i^j in equation (3).

The term $(c/f)(\Phi_i-\Phi^j-N_i^j)$ in (3) is called the (metric) carrier phase ambiguity. This term is constant in case of continuous tracking of the satellite. It can contain occasional jumps however, caused by temporary blockage of the signals or by weak signals. If jumps occur, they are usually equal to an integer number of cycles and then a cycleslip is said to have occurred.

The carrier phase ambiguity introduces an unknown for each satellite which is being tracked. Phase measurements are therefore not suitable for instantaneous single point positioning. This in contrast with the pseudo range observable. Phase measurements can be used in principle however for *static* single point positioning. That no actual static single point positioning applications can be found for the phase measurements, is due to the fact that in this case no advantage can be taken from the very high precision of the phase observable (the additional uncertainties in the clocks, the ephemeris and atmosphere, prohibit high precision single point positioning) and also that relatively long observation times are needed to determine the single carrier phase ambiguities (which makes it an unattractive method for the navigator).
The key to making a successful use of phase measurements lies in the concept of relative positioning. Geodesists and surveyors were the first to realize that relative positioning enables one to eliminate or greatly reduce the errors listed above, and therefore obtain position data in the centimeter-level or better which is required for most geodetic and geophysical applications. The next chapter is devoted to the different concepts of relative GPS positioning.

3. RELATIVE POSITIONING WITH GPS

Relative positioning with GPS involves simultaneous observation of a group of satellites by a minimum of two ground receivers. Several different methods of static and kinematic surveying with GPS have been developed over the past several years [5-9].

By GPS surveying we mean the high-precision determination of relative positions primarily based on GPS carrier phase measurements with resolved carrier phase ambiguities. In this chapter we will first review some of the existing concepts of GPS surveying, and then consider real-time applications. In order to show when and how the various errors listed in the previous section get eliminated or greatly reduced with relative positioning, we will use the linearized (metric) phase observation equation as our starting equation. It reads:

$$(4) \quad \Delta P_i^j = -\mathbf{e}_i^j * \Delta\mathbf{r}_i + \mathbf{e}_i^j * \Delta\mathbf{r}^j + c(\delta t_i - \delta t^j) + T_i^j - I_i^j + (c/f)(\Phi_i - \Phi^j - N_i^j) \ ,$$

with $\mathbf{e}_i^j$ the unit vector directed from receiver i to satellite j. With the phase ambiguity absent and a change in sign for I_i^j, equation (4) may also be read as the linearized pseudo range observation equation.

3.1. Static GPS surveying

Static relative positioning with GPS involves simultaneous observation of a group of satellites by a network of ground receivers that remain stationary at the occupied stations until all observations have been completed. The parameters of primary interest are the coordinate differences between the GPS receiver antennas. The remaining parameters are in a sense nuisance parameters. In order to understand why relative positioning enables one to determine the parameters of interest almost free from any interfering uncertainties such as ephemeris-, clock- and atmospheric effects, consider two receivers 1 and 2 simultaneously observing the same satellite j. Then two equations of the form (4) can be written. From these two equations the single difference phase observation equation, defined as $S_{12}^j = P_1^j - P_2^j$, can be formed (figure 7a),

$$(5)\quad \Delta S_{12}^j = \mathbf{e}_2^{j*}\Delta\mathbf{r}_{12} + (\mathbf{e}_1^j-\mathbf{e}_2^j)^*\Delta\mathbf{r}_1^j + c(\delta t_1-\delta t_2) + T_{12}^j - I_{12}^j + (c/f)(\Phi_1-\Phi_2-N_{12}^j)\ ,$$

with $\Delta\mathbf{r}_{12}$ the increment of the baseline vector $\mathbf{r}_{12} = \mathbf{r}_2-\mathbf{r}_1$.
The principal advantage of relative positioning now becomes apparent from this single difference observation equation. If we read equation (5) from right to left, the following remarks are in order.

a) *Phase ambiguities and clock errors:*
First we note that the single difference of the two phase ambiguities is free from the unknown initial transmitted phase Φ^j. The single difference is also free from errors in the satellite clock δt^j. This implies that the single difference also counters the frequency dithering effect of SA. The major issue of frequency dithering is however the impact it has on real-time positioning applications (see section 3.4). Furthermore, the unknown initial phases and clock terms of the two receivers get eliminated, if the difference of two single differences is taken. This difference is known as the double difference and it is defined as $D_{12}^{jk} = S_{12}^j - S_{12}^k$ (figure 7b). A double difference can be formed once the two receivers observe two satellites j and k at the same time. It only depends on the receiver-satellite geometry and on

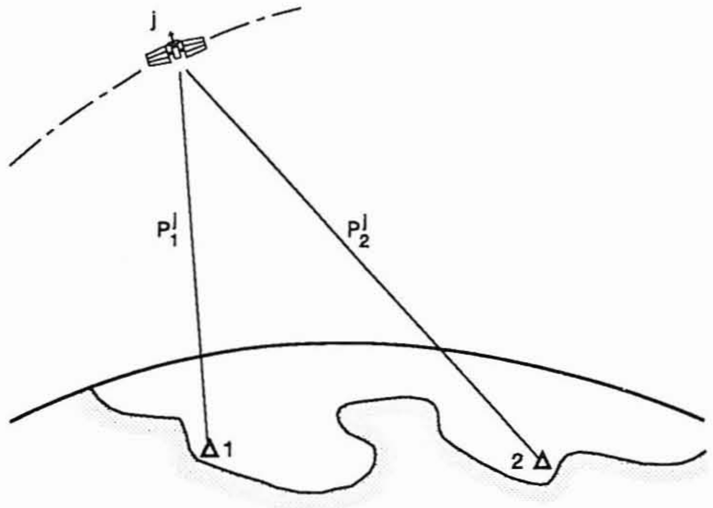

Figure 7a: The single difference phase observable

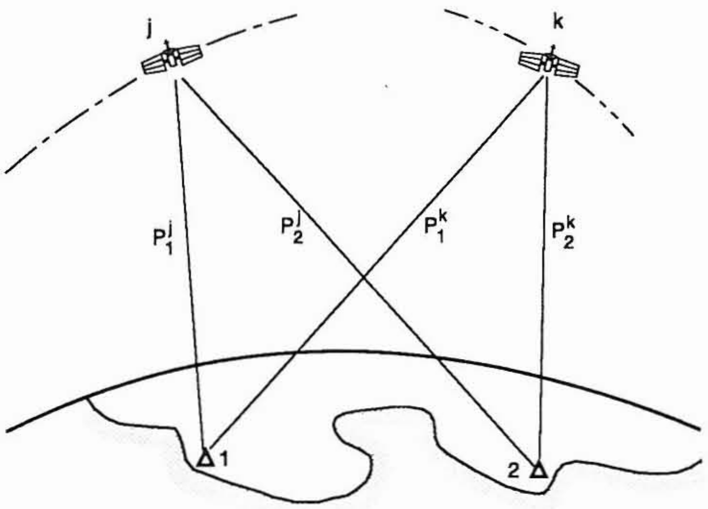

Figure 7b: The double difference phase observable

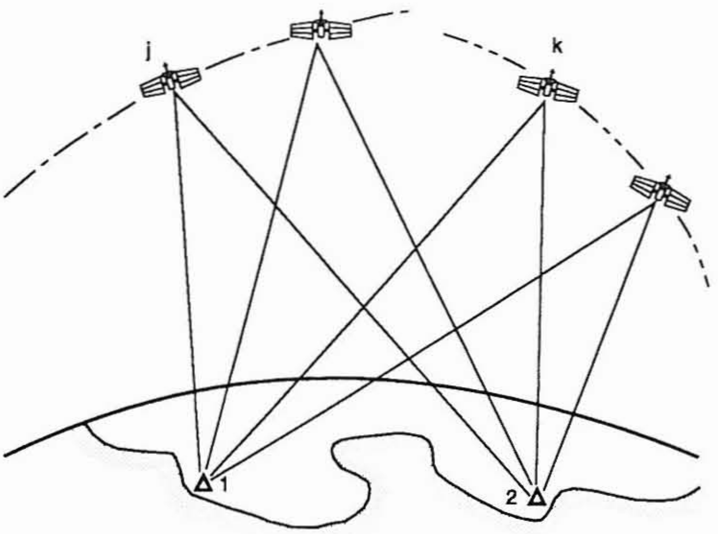

Figure 7c: The triple difference phase observable

the *integer* double difference phase ambiguity. Finally a triple difference, $D_{12}^{jk}(t+1)-D_{12}^{jk}(t)$, can be formed as the difference of two double differences for two different epochs (figure 7c). The unknown integer N-ambiguities get eliminated in the triple difference, provided that no cycleslips have occurred. The triple difference is therefore sometimes used as a first diagnostic to infer whether cycleslips have occurred or not.

b) *Tropospheric and Ionospheric delay:*
Let us now consider the difference in the atmospheric delays. For two receivers located close together, the atmospheric delays are the same because the radio signals travel through the same portion of the atmosphere and thus experience the same changes in velocity and ray bending. Hence the atmospheric delays cancel in the difference for small interstation distances. For longer interstation distances and high-precision applications however, these tropospheric and ionospheric delays have to be taken into account.
For high-precision applications the tropospheric delay cannot be determined accurately enough from empirical models (this is mainly due to the difficulties one has with modelling the "wet" path delay). The approach usually taken in a GPS network adjustment is therefore to treat the tropospheric parameters as unknowns in the adjustment and solve for them together with the geometric unknowns. In spite of the success of this approach, for GPS networks in regions of high "wet" path delay and high variability, tropospheric calibration is still the most important error source for larger baseline lengths. For a baseline of 100 km the troposphere can cause an error in the order of several centimetres [10,11].
The situation with the ionospheric delay is fortunately less problematic as with the tropospheric delay. For typical surveying applications where the interstation distance is less than 20-30 km, the ionospheric delay largely cancels in the single difference phase observable. This implies that for small interstation distances single frequency receivers suffice. For longer distances however, it is necessary to use dual-frequency receivers to overcome the ionospheric delay.
Fortunately carrier phase observations can be made on both the L_1 and L_2 frequency. If we denote the frequencies and phase observables for L_1 and L_2 as f_1, f_2 and $\phi_{i,1}^{j}$, $\phi_{i,2}^{j}$ respectively, then the linear combination

$$- \frac{f_1^2}{f_1^2-f_2^2}\,\phi^j_{i,1} + \frac{f_1 f_2}{f_1^2-f_2^2}\,\phi^j_{i,2}\ ,$$

is free from ionospheric effects. Thus this linear combination of two carrier phase observables can be used to eliminate the ionosphere if dual-frequency receivers are available.

Examples of high precision dual-frequency solutions are given in table 3 for the baseline Delft-Kootwijk. These dual-frequency results were obtained in the period 268-282 of 1989. The solution of each day is based on a three hour observation period.

Day	Δx (mtr)	Δy (mtr)	Δz (mtr)
268	25480.234	-95619.943	-13171.863
269	.307	.948	.820
271	.156	.950	.878
274	.253	.969	.837
275	.217	.924	.873
276	.100	-95620.013	.944
278	.097	.004	.935
280	.258	-95619.924	.852
281	.258	.909	.853
282	.239	.948	.854
	$\sigma_{\Delta x}$=0.071	$\sigma_{\Delta y}$=0.034	$\sigma_{\Delta z}$=0.040

Table 3: Baseline Delft-Kootwijk, dual-frequency solutions

c) *Satellite ephemeris:*

The increment vector $\Delta\mathbf{r}^j_1 = \Delta\mathbf{r}^j - \Delta\mathbf{r}_1$ in the inner product $(\mathbf{e}^j_1-\mathbf{e}^j_2)^*\Delta\mathbf{r}^j_1$ of equation (5), contains the vectorial difference of the uncertainties in the positions of satellite j and receiver 1. When the two receivers are located close enough together, the two unit vectors $\mathbf{e}^j_1$ and $\mathbf{e}^j_2$ can be considered identical, which implies the vanishing of $(\mathbf{e}^j_1-\mathbf{e}^j_2)^*\Delta\mathbf{r}^j_1$. Thus in applications where the stations are not too far apart, uncertainties in the satellite ephemeris cancel in the single difference. Therefore also the SA-induced manipulation of the satellite ephemeris cancel.

If we make the approximation that $\|\mathbf{r}_1^j\| = \|\mathbf{r}_2^j\| = 20000$ km (≅ GPS altitude), then

$$(6) \qquad (\mathbf{e}_1^j-\mathbf{e}_2^j)^*\Delta\mathbf{r}^j = \{\|\mathbf{r}_{12}\|/20000\}.\|\Delta\mathbf{r}^j\|.\cos\alpha.$$

This result can be used as a rule of thumb to infer the effect of uncertainties in the satellite ephemeris. For an interstation distance of $\|\mathbf{r}_{12}\| = 100$ km and an uncertainty of $\|\Delta\mathbf{r}^j\| = 20$ mtr in the satellite position, the effect equals for $\alpha = 0$: $(\mathbf{e}_1^j-\mathbf{e}_2^j)^*\Delta\mathbf{r}^j = 10$ cm (see figure 8).

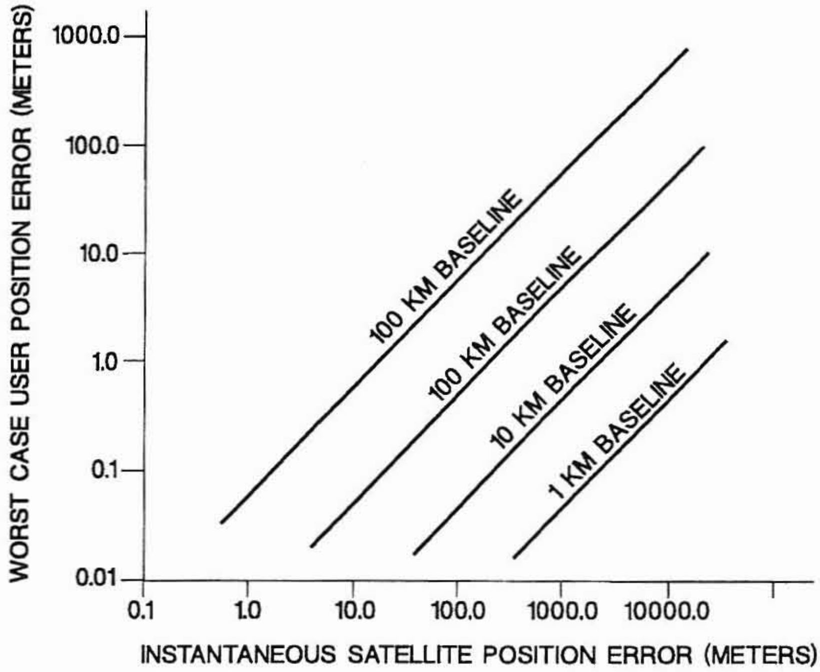

Figure 8: Baseline errors versus satellite position errors

The GPS ephemeris available today are of such quality that 1-2 ppm can be achieved. If higher accuracy is required over longer distances, it becomes necessary to take the disturbing forces of the satellite orbit into account. The main disturbances for GPS satellites are the nonspherity of the earth gravitational potential, the attraction of the sun and moon, and the solar radiation pressure. Because GPS satellites are at a high altitude the gravitational attraction can be accurately computed from a low-order spherical harmonic expansion of the gravity field. Also the accelerations caused by soon and moon can be accurately computed. Only the small but accumulating effect of solar radiation pressure needs to be estimated separately. A relatively simple way of dealing with orbital uncertainties would then consist of treating the Keplerian elements of the orbital equations of motion and their time derivatives, together with solar radiation parameters as unknowns in the static GPS-survey adjustment. This simplified approach has been shown to produce results that are already an order better than the 'orbit-fixed' approach. In the sections following we will assume, however, that the orbits can safely be taken as being fixed.

In Europe work is presently underway in employing the highly precise three dimensional positioning capabilities of GPS for establishing a common and uniform 3-dimensional continental geodetic reference frame. Currently, each country has its own reference frame and its own official plane cartographic representation system which were adopted at different dates during the 19th and 20th centuries. World War II revealed military requirements for a unique reference and cartographic representation system. This resulted in the development of the European Geodetic Network based on a framework of national 2-dimensional terrestrial networks (European Datum 1950, ED-50) and the 1-dimensional European Levelling Network (REUN). Later, RETrig (Readjustment of the European Triangulation), a sub-commission of the International Association of Geodesy (IAG), resumed those operations and provided the ED-79 and ED-87 scientific networks (see figure 9). Since 1987, the RETrig sub-commission has been replaced by the EUREF (EUropean REference Frame) sub-commission which aims at continuing those operations using geodetic space-techniques for establishing a European 3-dimensional reference frame. This will enable one to connect the traditional horizontal and vertical networks and to determine the transformation parameters between the various reference frames. A first large scale European GPS-campaign was organised by the EUREF sub-commission in May 1989, in which most of the West-European countries participated (see figure 9). The data of this first campaign, which covered 91 stations with interstation distances of some 100 km, is presently in the final state of processing and analysis. The processing and analysis of the scientific data of this campaign is done by various geodetic computing centres such as the LGR.
In the Netherlands, the NEREF (NEtherlands REference Frame) sub-commission of the Netherlands Geodetic Commission initiated in 1991 activities for the establishment of a GPS-based national 3-dimensional reference frame. In April 1991 a Dutch GPS-campaign, covering 15 stations in the Netherlands, was organised for the densification of the EUREF-network. The processing and quality control of this campaign is done in close collaboration between the LGR and the surveying departments of he Dutch Cadastre and the

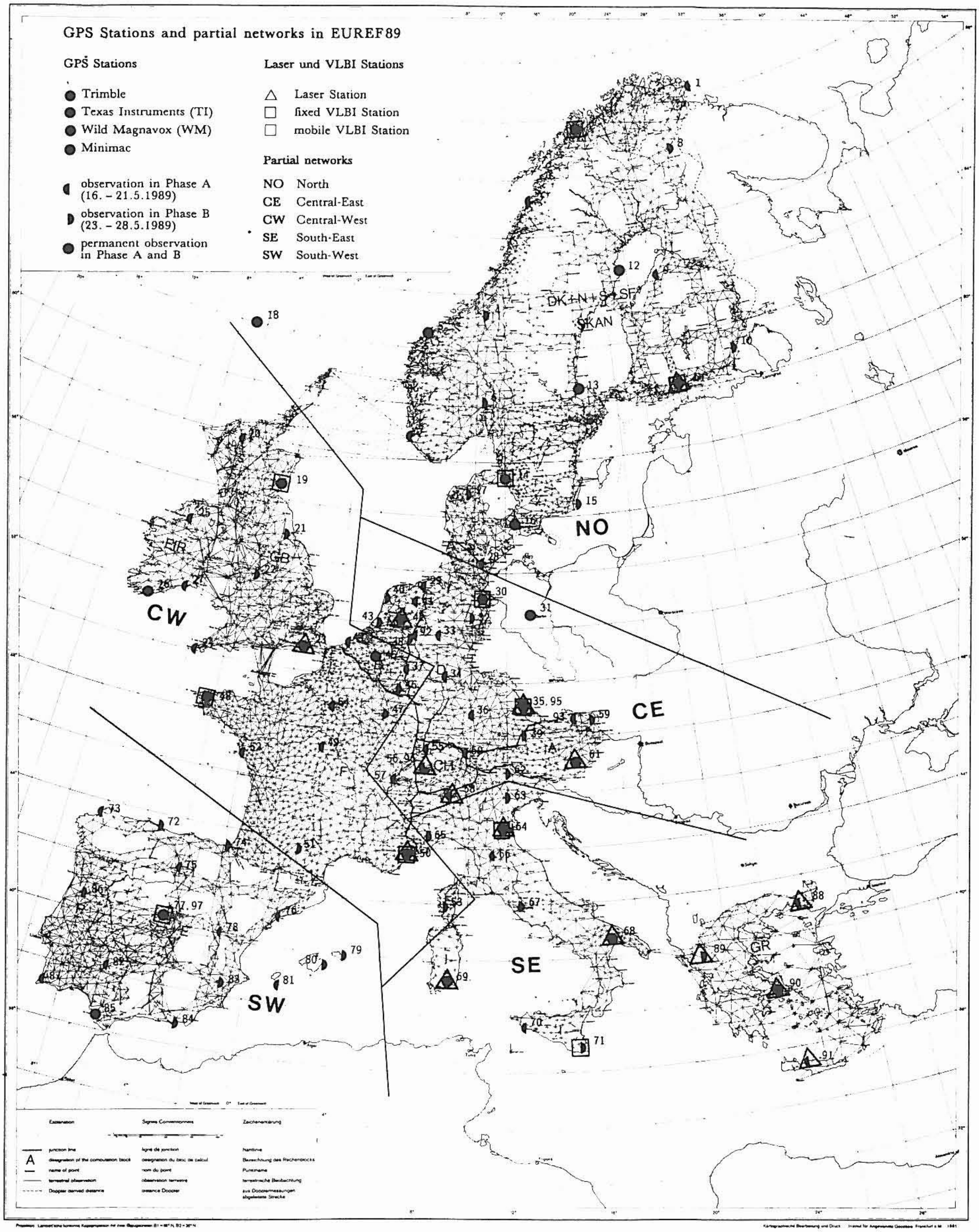

Figure 9: ED-87 and EUREF-89

Rijkswaterstaat. Densification of this NEREF-network up to interstation distances of some tens kilometres is expected to take place in the near future so as to enable GPS-users to tie their local measurements to the NEREF-network and subsequently to the EUREF-network.

3.2. Semi-kinematic GPS surveying

Since the introduction of GPS-based surveying techniques, the aspect of productivity, especially for small scale applications, has become very important. All techniques proposed so far to improve productivity have one basic objective in common, namely to reduce the observation time to determine the station coordinates. In GPS-surveying, the reduction in observation time is primarily hindered by the time required to determine the phase ambiguities to a sufficient precision (σ=30mm). Since GPS satellites are in very high altitude orbit, their relative position with respect to the receiver changes slowly. As a result long observation times are necessary to yield the required variation in satellite-receiver geometry, which is needed to determine the individual phase ambiguities with sufficient precision.

The importance of the change in satellite-receiver geometry for the determination of the phase ambiguities is best explained by referring to the following linear(ized) system of equations:

$$(7) \qquad \begin{bmatrix} \mathbf{y}_1 \\ \mathbf{y}_2 \\ \cdot \\ \cdot \\ \mathbf{y}_k \end{bmatrix} = \begin{bmatrix} \mathbf{A}_1 & \mathbf{I} \\ \mathbf{A}_2 & \mathbf{I} \\ \cdot & \cdot \\ \cdot & \cdot \\ \mathbf{A}_k & \mathbf{I} \end{bmatrix} \begin{bmatrix} \mathbf{x} \\ \nabla \end{bmatrix} .$$

In this system of equations the k number of m-vectors $\mathbf{y}_i$ constitute the increments of the (double difference) phase observations of epoch i, the n-vector $\mathbf{x}$ contains the increments of the unknown coordinate differences between two stations, and the m-vector ∇ contains the unknown phase ambiguities. The satellite-receiver geometry at epoch i is contained in the design matrices $\mathbf{A}_i$ and the unit coefficients of the unknown phase ambiguities are contained in the unit matrices I. In the above linear system it is assumed that all satellites are continuously tracked during the whole period from epoch 1 to epoch k.

The linear system (7) consists of mxk number of equations in (m+n) unknowns. If we assume that mxk=(m+n), then the number of equations equals the number

of unknowns and one might be inclined to believe that the linear system is uniquely solvable for both $\mathbf{x}$ and ∇. This is however only the case if all the (m+n) number of column vectors of the coefficient matrix of system (7) are mutually *linear independent*. These column vectors are however certainly not linearly independent if the satellite-receiver geometry remains stationary, because then $\mathbf{A}_1=\mathbf{A}_2=..=\mathbf{A}_k$ holds. Of course, since the satellite-receiver geometry never remains stationary, a strict linear dependency will not exist. But, with a slow change in the satellite-receiver geometry, one will have $\mathbf{A}_1\simeq\mathbf{A}_2\simeq..\simeq\mathbf{A}_k$, implying that the linear independency is only weakly present. This then on its turn implies that the parameters of both $\mathbf{x}$ and ∇ are only poorly estimable. Hence, in order to be able to estimate $\mathbf{x}$ and ∇ properly, one will have to make sure that $\mathbf{A}_1\neq\mathbf{A}_k$. This is why long observation times are necessary to determine the phase ambiguities with sufficient precision. Typically it takes in the order of 20-30 minutes for very short baselines (less than 1km), and 2 to more hours for long baselines. The observation time increases with baseline length as a result of such unmodelled error contributions as atmospheric delay decorrelation, and differences in the multipath seen at the two antenna locations.
Semi-kinematic surveying is a method that tries to reduce the actual time required to visit a station. At present, there are basically three ways to execute a semi-kinematic survey:

1) With revisiting of stations:

It is known from experience of static GPS surveying that phase measurements over an observation period of one hour quarantee phase ambiguity resolution for short baselines (up to 10km). But the phase ambiguity resolution becomes critical in this case if only data for a timespan of, say, 10 minutes is available. This timespan is namely too short for noticing an appreciable change in satellite-receiver geometry. It is also known however that not all the data of the longer observation period contribute in the same manner to the determination of the phase ambiguities. Because of the relatively slow change in satellite-receiver geometry, only the first and last part of this period are instrumental in determining the phase ambiguities. The basic idea of this semi-kinematic GPS survey method is therefore to have at least two periods of carrier phase data collection at the same station in static mode for a few minutes each. These two data collection periods are separated by a time interval large enough (> 30 min) to yield appreciably different satellite-receiver geometry. During this time interval other survey stations

can be visited for similar brief observation periods.
In terms of our earlier linear system (7), the idea of this method is therefore to plan the survey such that instead of (7) the following linear system is obtained,

$$(8)\qquad \begin{bmatrix} y_1 \\ y_2 \\ \cdot \\ \cdot \\ y_k \end{bmatrix} = \begin{bmatrix} A_1 & & & I \\ & A_2 & & I \\ & & \cdot & \cdot \\ & & \cdot & \cdot \\ A_k & & 0 & I \end{bmatrix} \begin{bmatrix} x_1 \\ x_2 \\ \cdot \\ x_k \\ \nabla \end{bmatrix},$$

with $A_1 \neq A_k$, and where x_i denote the unknown coordinate differences of the stations visited by the mobile receiver. The fact that $A_1 \neq A_k$ holds, allows one to determine all the unknown parameters with a sufficient precision.
The advantage of this method is clearly that it reduces the total observation time considerably. The method does require however careful planning of the complete survey before execution.

2) Starting from a known baseline:
This method requires that in the vicinity of the survey area at least two stations with accurately known coordinates are available (5cm or better). The survey begins by placing the antennas of the two receivers over these two points. This preliminary occupation of a few minutes on two known points is needed to determine the integer phase ambiguities. After this initialization, the antenna of the second receiver is lifted and moved on to a new point whose coordinates need to be determined. It then remains over this new point for a period in the order of a few minutes, before it is picked up and moved again to another point. This process continues until all the unknown stations in the survey area have been occupied. In this way a small scale network may be surveyed with a precision comparable to that of static GPS.
In order to explain how use is made of the accurately known coordinates of the two stations for the fast and precise determination of the phase ambiguities, we refer to the following two linear(ized) systems of equations:

$$(9)\qquad \begin{bmatrix} y_1 \\ y_2 \\ \cdot \\ \cdot \\ y_k \end{bmatrix} = \begin{bmatrix} A_1 & & & I \\ & A_2 & & I \\ & & \cdot & \cdot \\ & & \cdot & \cdot \\ & & A_k & I \end{bmatrix} \begin{bmatrix} x_1 \\ x_2 \\ \cdot \\ x_k \\ \nabla \end{bmatrix}, \quad \begin{bmatrix} y_1 - A_1 x_1 \\ y_2 \\ \cdot \\ \cdot \\ y_k \end{bmatrix} = \begin{bmatrix} 0 & & & I \\ A_2 & & & I \\ & \cdot & & \cdot \\ & & \cdot & \cdot \\ & & A_k & I \end{bmatrix} \begin{bmatrix} x_2 \\ \cdot \\ x_k \\ \nabla \end{bmatrix}.$$

These equations again describe the linear(ized) relationships between the (double difference) phase observations $\mathbf{y}_i$ and the unknown coordinate differences $\mathbf{x}_i$ and unknown phase ambiguities ∇. And as before it is assumed that all satellites are continuously tracked. It will be clear from our previous discussion that the solution of the first linear system of equations of (9) suffers from a weak linear independency if $\mathbf{A}_1 \simeq \mathbf{A}_2 \simeq .. \simeq \mathbf{A}_k$. The solution of this system therefore lacks sufficient precision if the observation time is too short. This lack of sufficient precision can be circumvented either by means of prolonging the observation time, or by introducing additional information on the unknowns. When one starts the survey from a known baseline, it is this latter option which is chosen. With an accurately known baseline $\mathbf{x}_1$, the first linear system of (9) transforms to the second. And this system is indeed linear independent, even if $\mathbf{A}_1 \simeq \mathbf{A}_2 \simeq .. \simeq \mathbf{A}_k$; thus also for short observation times.

From the above it will be clear that continuous tracking of carrier phases of four or more satellites during the complete survey (including transport and positioning of antenna) is the essence of this method. Continuity in the carrier phase profile measured provides the user namely with an (almost) exact history of position changes of the moving antenna since leaving its initial position. It is therefore of importance that the antenna transport between the stations is done with the utmost care in order to avoid signal obstructions.

3) With antenna exchange:

Instead of relying on a known baseline, this method solves the problem of determining the integer phase ambiguities by the artifice of moving what is normally the stationary antenna to the initial position of the moving antenna while, at the same time, moving the mobile antenna from its initial position to the position of the stationary antenna. The implications of this 'antenna exchange' are best explained by referring to the double difference (metric) phase equation. Before the 'antenna exchange' the double difference phase equation reads (if we disregard atmospheric effects),

$$(10) \qquad D_{12}^{jk} = S_{12}^{j} - S_{12}^{k} = \|\mathbf{r}_1^j\| - \|\mathbf{r}_2^j\| - \|\mathbf{r}_1^k\| + \|\mathbf{r}_2^k\| + N_{12}^{jk} .$$

After the 'antenna exchange' the same double difference phase equation can be formed, with the important exception however that now the sign of the phase ambiguity has changed,

$$D_{12}^{jk} = S_{12}^{j}-S_{12}^{k} = \|\mathbf{r}_1^j\|-\|\mathbf{r}_2^j\|-\|\mathbf{r}_1^k\|+\|\mathbf{r}_2^k\|-N_{12}^{jk} \ . \tag{11}$$

This change in sign is due to the fact that the phase ambiguity is coupled with the antenna and not with the station over which the antenna is placed. From (10) and (11) follows that the sum of the two double differences is free from the integer phase ambiguity. Hence the very precise double differences can then be used to solve for the unknown baseline. Once the baseline is solved for, the unknown integer phase ambiguities can be determined and the survey proceeds as with the first method. Thus also here continuous tracking of the satellites is required. As with the previous method this has the drawback that in the event of loss of lock a re-initialization of the survey is needed [12].

In terms of our earlier linear system, the concept of the 'antenna exchange' can be explained by noting that it accomplishes the transformation of

$$\begin{bmatrix} \mathbf{y}_{11} \\ \mathbf{y}_{12} \\ \mathbf{y}_2 \\ \vdots \\ \mathbf{y}_k \end{bmatrix} = \begin{bmatrix} \mathbf{A}_{11} & & & \mathbf{I} \\ \mathbf{A}_{12} & & & \mathbf{I} \\ & \mathbf{A}_2 & & \cdot \\ & & \ddots & \cdot \\ & & \mathbf{A}_k & \mathbf{I} \end{bmatrix} \begin{bmatrix} \mathbf{x}_1 \\ \mathbf{x}_2 \\ \vdots \\ \mathbf{x}_k \\ \nabla \end{bmatrix} \quad \text{to} \quad \begin{bmatrix} \mathbf{y}_{11} \\ \mathbf{y}_{12} \\ \mathbf{y}_2 \\ \vdots \\ \mathbf{y}_k \end{bmatrix} = \begin{bmatrix} \mathbf{A}_{11} & & & \mathbf{I} \\ \mathbf{A}_{12} & & & -\mathbf{I} \\ & \mathbf{A}_2 & & \cdot \\ & & \ddots & \cdot \\ & & \mathbf{A}_k & \mathbf{I} \end{bmatrix} \begin{bmatrix} \mathbf{x}_1 \\ \mathbf{x}_2 \\ \vdots \\ \mathbf{x}_k \\ \nabla \end{bmatrix}$$

The first system lacks sufficient linear independency if $\mathbf{A}_{11} \simeq \mathbf{A}_{12} \simeq \mathbf{A}_2 \simeq .. \simeq \mathbf{A}_k$, whereas the second system is completely linear independent, even if $\mathbf{A}_{11} \simeq \mathbf{A}_{12} \simeq \mathbf{A}_2 \simeq .. \simeq \mathbf{A}_k$.

3.3. Kinematic GPS surveying

Kinematic surveying with GPS is in concept close to semi-kinematic surveying. Also kinematic surveying relies on continuous carrier phase tracking and aims at the determination of the position of a mobile receiver relative to a simultaneously observing stationary receiver at an a priori known location. There are however also some marked differences. Instead of determining the coordinates of a discrete set of network points, as is the case with semi-kinematic surveying, the aim of kinematic surveying is to determine the complete continuous *trajectory* of a moving platform. Also the precision requirements of the two methods differ. The typical precision requirement of semi-kinematic surveying lies in the range of 1 ppm or better, whereas the relative precision requirement of most kinematic surveying applications lies at or below the 1-mtr level. Typical applications of kinematic surveying are positioning of geodetic and geophysical sensors (airborne photogrammetry, airborne and shipborn gravimetry), hydrographic surveying, and inshore and river navigation (see table 1).

It will be clear that the precision requirements of kinematic surveying cannot be met by utilizing the GPS pseudo range measurements alone. Carrier phase measurements are therefore needed. The carrier phase measurements, however, can only be used, as we have seen in the previous section, if some accurate initial relative position has been established a priori, and as long as the receiver keeps track of the satellites. The approach of kinematic surveying is therefore to make use of both the pseudo range and carrier phase measurements simultaneously. In this way one can eliminate their individual drawbacks (for pseudo ranges: relatively low precision; for carrier phases: potential cycleslips) and obtain through least squares filtering an optimal estimate of the trajectory. The least squares filter in fact takes care of the smoothing of the less precise pseudo ranges through the very precise carrier phase observables.

The model used for the least squares filtering consists of two parts. A model of (linearized) observation equations, containing the pseudo range and carrier phase observables. And a (linearized) state space model, which describes the postulated dynamics of the moving platform including time-dependent characteristics of instrumental parameters, such as e.g. receiver clock errors. The data and the two models are combined using the principle of least squares, and in this way provide optimal estimates for position and velocity of the moving platform. The attainable precision for relative positioning using this approach are reported in the literature to be in the order of 1 mtr [14,15].

When we compare the above described two concepts of semi-kinematic and kinematic surveying, the following remarks can be made. The semi-kinematic survey is, as we have seen, essentially made up of two parts: the initialization, which is needed to determine the integer phase ambiguities, and the survey itself where the observed carrier phases are used to determine the history of position changes of the mobile receiver. In the concept of kinematic surveying on the other hand, where usually one of the receivers is located out at sea, in the air, or in space, the semi-kinematic initialization procedure is thought impossible. Therefore pseudo ranges are included to overcome possible deficiencies with the carrier phase observables. Thus in a way, the pseudo ranges take over the role played by the semi-kinematic initialization. As a result carrier smoothed pseudo ranges are obtained which, although an improvement over the pseudo-ranges, still lack the high precision of the carrier phase observables. The intriguing question now is, whether it is really required to have the initialization done for a *stationary* baseline. The key to the solution of this problem lies in the notion of redundancy. At the time when the different methods of initialization were proposed, it was indeed required to have a stationary baseline. This was however not so much because of the fact that the method itself required a stationary baseline, but more because of the incomplete GPS satellite constellation at that time. With four GPS satellites visible, one indeed has to assume that the baseline is stationary in order to be able to solve quickly for the integer phase ambiguities. But when more than four satellites are visible, the constraint of having a stationary baseline can be relaxed. In fact several authors have already claimed on the basis of analytical as well as simulation studies that fast integer ambiguity resolution in a kinematic environment becomes possible with the fully configured GPS constellation. The important implication of this result is that in the near future also kinematic surveying applications may take the full benefit of the very precise carrier phase observables [16,17,18].

3.4. DGPS navigation

The GPS-system was originally designed for high precision single point positioning to support military navigation needs. This was made possible through the use of the encrypted precise P-code signal. The positioning precision based on the unencrypted and less precise C/A-code signal was generally expected to be about 200 meters (1 sigma). It turned out however that civil and other unauthorized users were able to reach a positioning precision in the order of 20 mtr with the unencrypted C/A-code. This unexpected situation prompted the U.S. government to implement the program of Selective Availability (SA), which degrades the single point positioning precision based on the C/A-code to the level of 100 mtr (2 sigma). As a result of this, the importance of the concept of relative positioning was also soon recognized by the civilian navigation community.

The concept of DGPS-navigation is very close to the concepts of GPS surveying as previously discussed. The DGPS-navigation concept also involves the use of data from a stationary GPS receiver located in the vicinity of the GPS receiver-equipped users that allow certain errors common to mobile and stationary receivers to be removed from the user's position measurements. It is also expected, like with kinematic GPS surveying, that the stationary reference receivers will perform both carrier phase tracking as well as pseudo range code tracking. And the user can also utilize carrier phase tracking if required by the application.

The main difference between DGPS-navigation and the earlier discussed GPS surveying applications is however that the navigation applications require real-time processing of the data. This implies that the solutions derived at the stationary GPS receivers are continuously compared with the known surveyed location of these receivers and that on the basis of these comparisons correction terms are send to the user to allow him to improve his own position solution (figure 10).

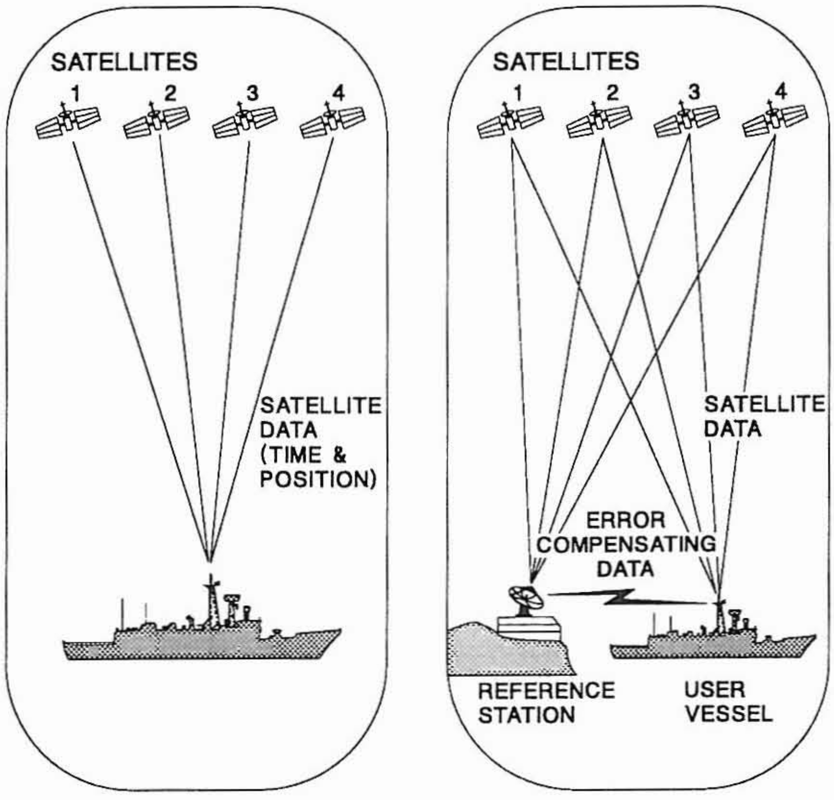

Figure 10: GPS and DGPS operation

Several implementations of the DGPS-navigation concept have been suggested.

1) *Coordinate corrections:*

The stationary reference receiver is placed at a known surveyed location and the differences between the known coordinates and the coordinates as

determined from the GPS measurements, are transmitted to the user. The user would then subtract these coordinate differences from his own estimated coordinates in order to eliminate the errors common to both receivers.
Although this approach is straightforward enough, it has one important drawback. The coordinate corrections are namely only valid as long as both receivers use the same set of satellites. This implies, if the user uses a satellite selection strategy which differs from the one used at the stationary receiver, that not all errors get eliminated in the differential solution.

2) *Pseudo range corrections:*
The stationary reference receiver is placed at a known surveyed location and the residuals in the pseudo range to all visible satellites are determined and transmitted to the user. In this case, there is no need for the user to use the same satellite selection strategy, since he is getting the corrections for all the satellites. The user then subtracts the pseudo range corrections from his own measured pseudo ranges prior to determining his navigation solution.

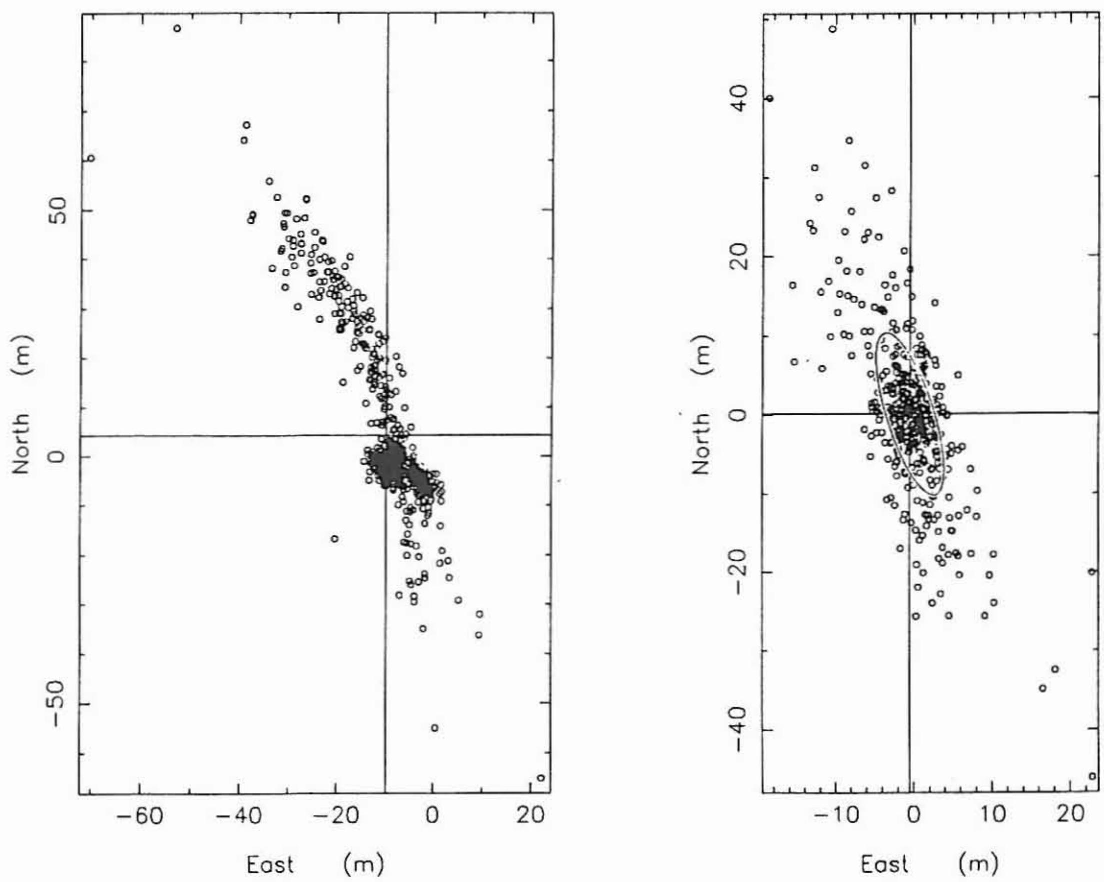

Figure 11: a) GPS scatterplot ; b) DGPS scatterplot

An example of the positioning inprovement obtained with DGPS (in the absence of SA) is shown in figure 11. Figure 11a shows a horizontal scatterplot of GPS single point positioning referenced with respect to the known location of the receiver in Delft. Note that the mean of the scatterplot is significantly biased and that the scattering of the horizontal position is rather inhomogeneous. This inhomogeneity is due to the switches in the combination of satellites that occurred during the three hours observation period. Figure 11b shows the corresponding horizontal DGPS scatterplot for the 100 km baseline Kootwijk-Delft. Note that the mean of the scatterplot is now practically free from any bias and that the scattering is distributed rather homogeneously. The elongation of both scatterplots and of the empirical point standard ellips of figure 11b is due to the receiver-satellite geometry during the observation period.

3) *Reference receiver acts as pseudo-satellite:*
This concept is an attractive extension of the previous one. The pseudo range corrections for all satellites are determined and included in the navigation message broadcast by the pseudo-satellite. The user can collect this information as part of the regular GPS navigation message and correct his own solution accordingly. Since the reference receiver acts as a pseudo-satellite the user can obtain an additional pseudo range measurement from the pseudo-satellite, thus strengthening the geometry of the satellite configuration [19].

When designing stationary reference stations for DGPS-navigation, there are two major issues that should be considered. The first one concerns the question how to deal with Selective Availability (SA). And the second issue concerns the configuration of the reference stations in relation to the area of effective coverage of the differential corrections.
We will first consider the effect of SA on DGPS-navigation operation. This aspect has been delt with by the RTCM SC-104 [20]. In contrast to the frequency dithering aspect of SA, the SA ephemeris manipulation can be disregarded in DGPS-navigation operations. The ephemeris manipulation causes namely only slowly varying errors. They therefore cancel in case of relative positioning when the pseudo range corrections are send with an update rate of a few minutes or so. Frequency dithering however is intended to degrade velocity information, and causes the pseudo ranges to vary quickly with a period in the range of minutes. An update rate of a few minutes is therefore

inadequate, since the precision of the correction degrades as it gets older. Originally, the standard DGPS-navigation operation was based on sending pseudo range corrections only. But since the SA range rate error standard deviation is believed to be about 0.14 mtr/sec, and the acceleration error standard deviation about .0037 mtr/sec^2 [21], this would imply with a typical 1-sigma zero-delay differential pseudo range error of 1 mtr, that the differential pseudo range standard deviation would be 2 mtr after a 12 sec delay, 3 mtr after a 20 sec delay and 4 mtr after a 28 sec delay. With the fully configured GPS constellation, having an average HDOP of 1.5 (the HDOP rarely exceeds 2 for an minimum elevation angle of $\varepsilon=10^o$), this translates in an average 1-sigma horizontal radial position error of 7 metres after 30 seconds. Thus a 1-sigma positional change of about 0.2 metres per second. This relatively fast growth in positioning error would require a too high update rate for the pseudo range corrections. In order to lower the required update rate, the RTCM SC-104 therefore decided to add a range-rate correction to the standard differential correction message [22]. The total correction therefore now takes the form,

$$\Delta p(t) = \Delta p(t_o) + \Delta\dot{p}(t_o)(t-t_o) \ ,$$

where $\Delta p(t)$ is the correction to be applied, $\Delta p(t_0)$ is the pseudo range correction from the message, $\Delta\dot{p}(t_o)$ is the pseudo range rate correction from the message, and t_o is the time reference of the correction. The corrections $\Delta p(t_o)$ and $\Delta\dot{p}(t_o)$ are determined at the reference station from pseudo range and carrier phase measurements. By eliminating the SA range rate uncertainty, the remaining growth in positioning error is due to the SA induced range acceleration uncertainty and the precision with which the range rates can be determined. Figure 12 shows the remaining DGPS-navigation error growth due to SA. For the 1-sigma horizontal radial position error due to SA to stay under 1.6 metres, the transmission rate must exceed 20 seconds.

The second major issue of DGPS-navigation operation concerns the effective area of coverage of the differential corrections. As we have seen above, DGPS-navigation is a means for improving navigation accuracy in a local area. However, as the distance between user and the stationary reference station increases, range decorrelation (mainly due to uncertainties in satellite ephemeris and atmospheric delays) occurs and the accuracy degrades (figure 8). One way to enlarge the effective area of coverage would simply be to place more than one single operating DGPS-station in the area of interest.

This should be done in such a way that the effective areas of coverage of the individual DGPS-stations show enough overlap. In this way the user located at the perimeter of the effective area of coverage of 'his' DGPS-station is given the opportunity to switch from 'his' DGPS-station to the following DGPS-station.

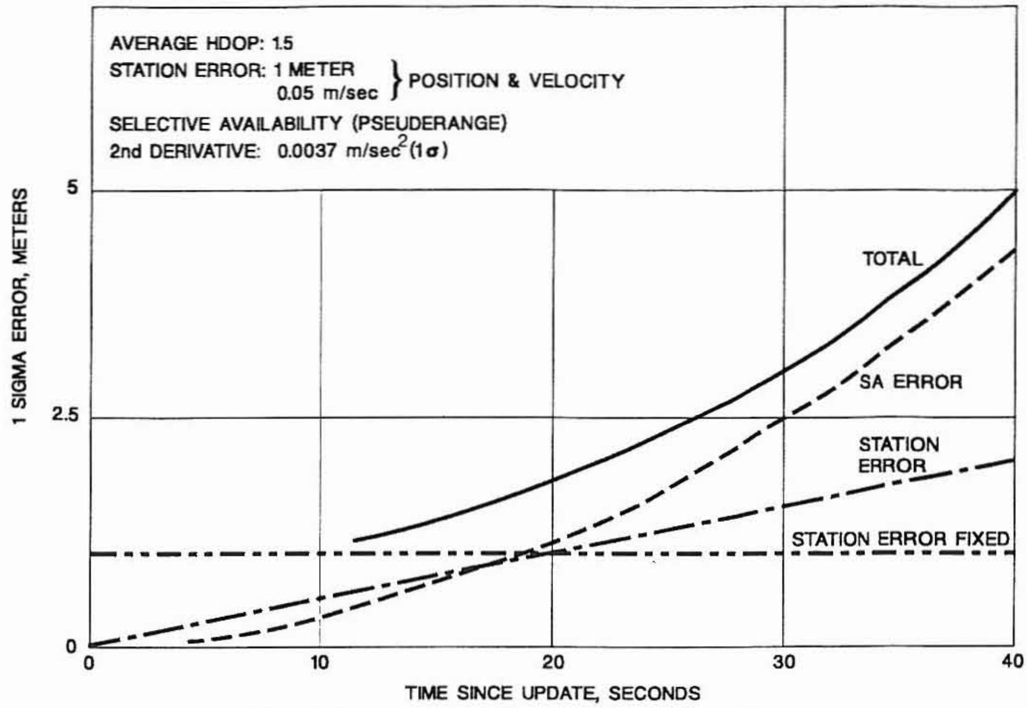

Figure 12: DGPS-navigation error growth due to SA

Although this simple approach indeed enlarges the effective area of coverage it has some fundamental drawbacks. First of all it can be expected that the user will experience unacceptable inhomogeneities in his navigation solutions when switching from one DGPS-station to another. This is very similar to what has been experienced on the North Sea at the time when Doppler-derived positions had to be connected to the ED-50 reference system [23]. Secondly, since the user is only making use of the various DGPS-stations on a 'one-at-a-time' basis, he is in fact not getting the most out of the system. The correct approach for enlarging the effective area of coverage is therefore to design, as is common practice in GPS-surveying, an *integrated network* of stationary GPS reference stations. Such a network is composed of one master GPS reference station and several local slave stations. Each local slave station is equipped with a GPS receiver and a high quality clock. These stations track all the satellites that are within the field of view, and sent their GPS measurements to the master station. At the master station all the incoming data is processed to obtain one unique set of corrections. These error corrections are then transmitted via a communication link to the users. In a way this concept allows the GPS receiver of the user to act as a digitizer (figure 13).

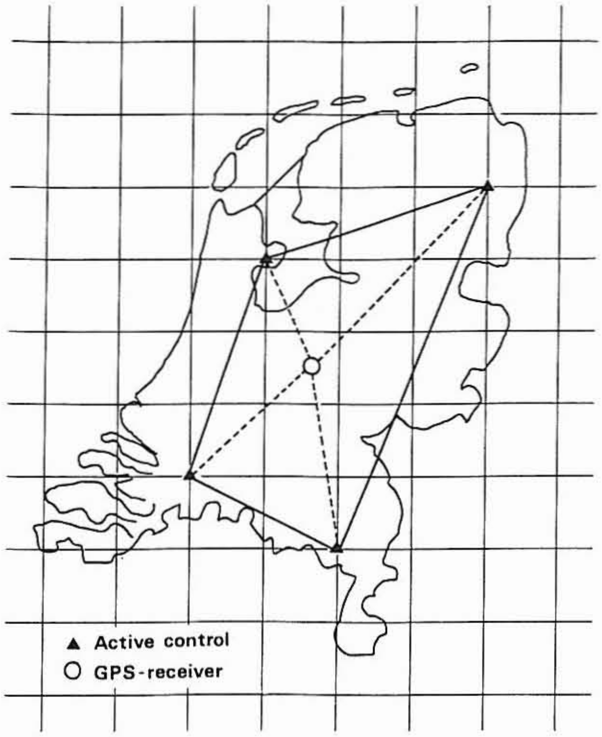

Figure 13: The GPS digitzer concept

The advantages of this integrated network approach over the previous discussed approach are:

1) The transmitted differential corrections are consistent within the area covered by the network, and they do not contain inhomogeinities.
2) With the same number of GPS reference stations, the integrated network approach allows one to cover a larger effective area. The network approach enables one namely to include orbital relaxation techniques.
3) Due to the increase in redundancy, the ability to exercise quality control improves considerably with an integrated network approach.

It can therefore be expected that for navigation applications requiring higher accuracies and larger effective areas of coverage, the above described integrated network approach, which is identical in concept to the existing surveying concepts of geodetic networks, will indeed replace existing DGPS-navigation operations.

4. QUALITY CONTROL

4.1. Introduction

In surveying the quality of a network is considered to be made up of three factors: Economy, Precision, and Reliability [24]. *Economy* expresses the total cost of designing, measuring, adjusting and validating the survey network. Network *precision*, as described by the a posteriori covariance matrix of the network coordinates, expresses the network's characteristics in propagating random errors (figure 14a). And *reliability*, as described by the minimal detectable biases, expresses the ability of the redundant observations to detect and identify specific modeling errors (internal reliability, figure 14b) together with the network's characteristics in propagating these modeling errors (external reliability).

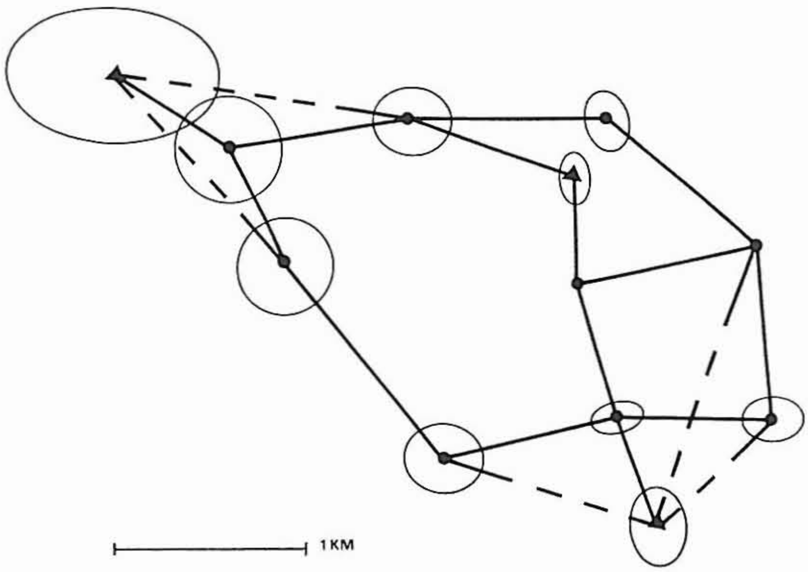

Figure 14a: Precision: small survey network with point standard ellipses

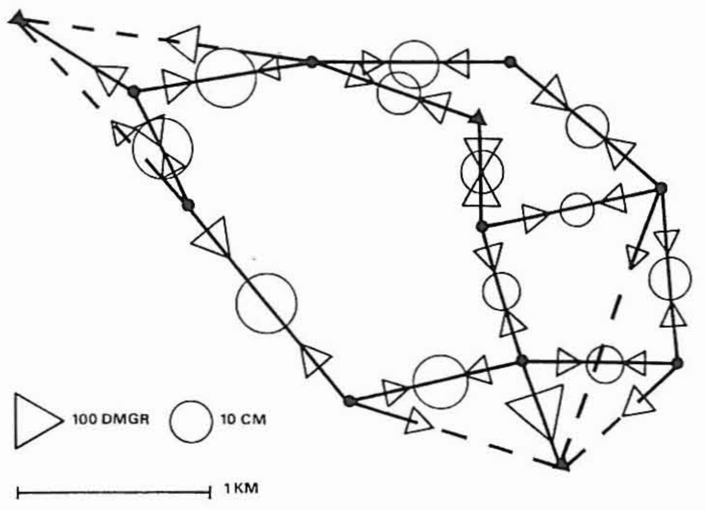

Figure 14b: Reliability: small survey network with internal reliability

The problem of quality control in survey networks can thus be said to be the problem of designing and measuring a precise and reliable enough network which can also be realized in an economical way. As such it is a multi-objective optimization problem for which the quantification of the criteria that should be fulfilled follow from the purposes the network should serve.

In this chapter we will give a very brief review of the *quality control theory* as developed at the Delft Geodetic Computing Centre (LGR). The theory has already been used extensively in the last fifteen years for a variety of applications in the fields of geodesy, surveying, photogrammetry and navigation. It has been used in deformation analysis for the detection and identification of possibly conflicting hypothesized geophysical models [25,26]. In surveying and photogrammetry the theory has been used for the detection and identification of outliers and for the design of general purpose geodetic networks [27-29]. And more recently the theory has been generalized for use in integrated navigation systems. It consists of a recursive DIA-procedure for the detection, identification and adaptation of navigational model errors. The DIA-procedure is based on uniformly-most-powerful teststatistics and can be executed in real-time [30-32].

In order to explain the basic concepts of the quality control theory, we will restrict ourselves in the following to the rather simple GPS single point positioning model, and only discuss some of the aspects of testing and reliability. The application to GPS-based civil aviation is briefly described. Applications of the theory to GPS survey networks and to GPS-based integrated navigation applications are however not discussed. For these applications the reader is referred to [33,34].

4.2. On GPS-based civil aviation quality monitoring

An important application of the quality control theory can be found in the area of GPS-based navigation for civil aviation. GPS has the potential to provide significant navigation system benefits for civil aviation users due to its superior performance in terms of precision and coverage over the current ground-based radio navigation systems. However, stringent safety requirements must be met for GPS to receive U.S. Federal Aviation Administration (FAA) approval for use in the U.S. airspace. To assure the safety of the aircraft, a timely warning is required any time the performance of the GPS based navigation system fails to meet the accuracy requirements applicable to the particular phase of the flight of the aircraft. Although the Global Positioning System itself has extensive built-in features and operating procedures to ensure the integrity of the navigation service, the delay inherent in the GPS Control Segment monitoring does not meet the requirements of timely notification of system failures [35]. Therefore other means have to be identified to ensure the quality of the GPS navigation service. There are basically three approaches that can be considered, either separately or in support of each other:

1) *GPS Integrity Channel:*

With a GPS Integrity Channel (GIC), a ground-based GPS monitoring system is used to track the GPS signals and monitor the GPS satellite errors. This approach is therefore essentially based on the integrated network concept as discussed in section 3.4. A concept for a GIC network is shown in figure 15 [36]. In this concept the master station uplinks the GIC data to geostationary satellites, which then re-broadcasts it to users in the area covered. Although the GIC concept would provide for a highly effective monitoring service, it also requires a significant investment in ground equipment, satellite communication links and customized receivers for all aircraft subscribing to the service.

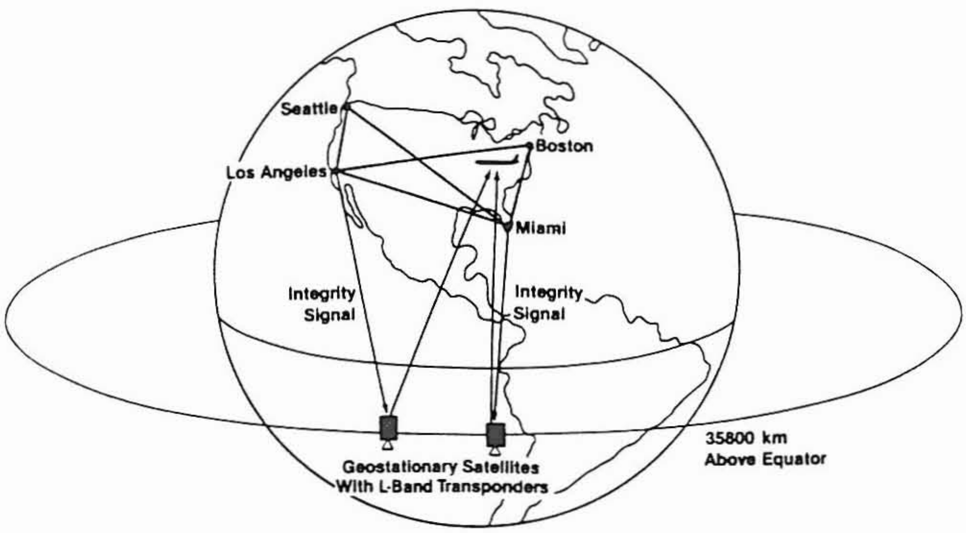

Figure 15: GIC network for North America [36]

2) *Integrated systems:*

By integrating GPS with other navigation sensors it is possible to improve the overall navigation performance while ensuring quality due to the additional redundancy [33]. There exists a variety of navigation sensors that may be used to aid the GPS system. Potential candidates are a.o.: baro-altitude aiding, integration of GPS with inertial systems, and GPS/Loran-C integration. A GPS receiver integrated with a barometric altimeter and/or an inertial unit can meet the requirements for an en route oceanic flight. And a GPS/Loran-C integrated system would provide sufficient redundancy to meet the requirements for en route, terminal and non-precision approaches wherever there is adequate Loran-C transmitter coverage. But, according to [37]. the most promising integrated system would be a GPS/Glonass receiver. It has the potential of providing global navigation suitable for all phases of the flight.

3) *Receiver Autonomous Integrity Monitoring:*
When the GPS receiver tracks more than four satellites, redundant information becomes available that can be used to validate the health and error levels of the individual satellite signals. Receiver Autonomous Integrity Monitoring (RAIM) is the name coined by the FAA for methods that achieve this objective. It is the simplest and most cost effective way for monitoring the quality of GPS. It will be discussed in the sections following.

4.3. Detection and identification

The mathematical model:
If we assume GPS single point positioning based on pseudo ranges, the (linearized) observation equations of the GPS measurements can be cast in the following system of equations:

$$\underline{\mathbf{y}} = \mathbf{A}\mathbf{x} + \underline{\mathbf{e}}\ , \tag{12}$$

where; $\underline{\mathbf{y}}$: is the mx1 random vector of pseudo range increments (the underscore indicates randomness),

$\mathbf{A}$: is the mx4 (linearized) design matrix, consisting of the line-of-sight unit vectors to the satellites with 1's in the fourth column corresponding to the unknown receiver clock error,

$\mathbf{x}$: is the 4x1 vector of unknown parameters, containing the increments of the three position coordinates and one receiver clock parameter: $\mathbf{x} = (\Delta x, \Delta y, \Delta z, \delta t)^*$,

$\underline{\mathbf{e}}$: is the mx1 random vector of a-priori pseudo range residuals, which will be assumed to be normally distributed.

The a-priori residuals are also assumed to have a zero mathematical expectation and known covariance matrix $\mathbf{Q}$:

$$E\{\underline{e}\} = \mathbf{0} \quad ; \quad D\{\underline{e}\} = \mathbf{Q} \, . \tag{13}$$

The equations (12) and (13) constitute our null-hypothesis H_o. Under this null-hypothesis, the best (in the sense of minimal variance) linear unbiased estimator of the unknown parameter vector $\mathbf{x}$ is known to be given by the following least-squares estimator:

$$\hat{\underline{\mathbf{x}}} = (\mathbf{A}^*\mathbf{Q}^{-1}\mathbf{A})^{-1}\mathbf{A}^*\mathbf{Q}^{-1}\underline{\mathbf{y}} \, . \tag{14}$$

This result is used for computing the navigation solution. The precision of the estimator $\hat{\underline{\mathbf{x}}}$ is described by its covariance matrix, $\mathbf{Q}_{\hat{\mathbf{x}}} = (\mathbf{A}^*\mathbf{Q}^{-1}\mathbf{A})^{-1}$.

Validation of the mathematical model:
The least-squares estimator (14) is an optimal estimator with well defined statistical properties. The optimality of this estimator is however only guaranteed as long as the assumptions underlying the mathematical model H_o hold. Misspecifications in the model due to e.g. outliers or sensor failures, will invalidate the results of estimation and thus also any conclusion based on them. It is therefore of importance to have autonomous means of monitoring the quality of the assumed mathematical model H_o. This quality monitoring is based on the execution of statistical tests. Our testing procedure consists of three steps: detection, identification, and adaptation. Adaptation, as is needed in case of recursive least-squares filtering will not be considered here, but see [38].

Detection:
The objective of the detection step is to test the overall validity of the assumed mathematical model H_o. It will be assumed that any violation of H_o is restricted to the functional part of the model. In other words, the stated random characteristics of the stochastic vectors are assumed to remain valid. Since violation of the functional part of the model implies that $E\{\underline{\mathbf{y}}\}$ is not an element of the range space of the design matrix $\mathbf{A}$, the null-hypothesis H_o is opposed to a more relaxed alternative hypothesis H_a in which more explanatory variables are included. For detection the most relaxed

alternative hypothesis H_a is chosen: $E\{\underline{y}\} \in R^m$. It can be shown that the uniformly-most-powerful teststatistic for testing H_o against H_a is given by the following quadratic form:

$$\underline{T} = \hat{\underline{e}}^* Q^{-1} \hat{\underline{e}} \ ,$$

where $\hat{\underline{e}}$ is the random vector of least-squares residuals.
The teststatistic $\underline{T}$ is distributed under H_o and H_a as: $\underline{T}|H_o \simeq \chi^2(m-4,0)$ and $\underline{T}|H_a \simeq \chi^2(m-4,\lambda)$, with noncentrality parameter λ. The detection step now consists of comparing, at the level of significance α, the sample value of $\underline{T}$ with the critical value $\chi^2_\alpha(m-4,0)$ of the χ^2-distribution. The null-hypothesis H_o is rejected if the sample value of $\underline{T}$ exceeds the critical value; otherwise the null-hypothesis is accepted. This concludes the detection step.

Identification:
After a model error has been detected, identification of the potential source of the model error may be needed. If this is the case, one has to perform a search among the candidate hypotheses for the most likely alternative hypothesis. Hence, for identification candidate alternative hypotheses need to be specified explicitly. This specification is non-trivial and probably the most difficult task in the process of quality control. It depends to a great extend on experience and ones knowledge of the navigation system. For the present discussion we will restrict ourselves to the so-called *conventional* alternative hypotheses H_{ai}. With the conventional alternative hypotheses it becomes possible to screen the individual observables one-by-one for the presence of outliers. This implies that only one additional explanatory variable is needed for each conventional alternative hypothesis. Under the assumption that the observables are mutually uncorrelated, the uniformly-most-powerful teststatistic for testing for the presence of an outlier in the i^{th} observable, reads:

$$\underline{w}_i = \hat{\underline{e}}_i / \sigma_{\hat{e}_i} \ .$$

The teststatistic $\underline{w}_i$ is normally distributed under H_o and H_{ai} as: $\underline{w}_i|H_o \simeq N(0,1)$ and $\underline{w}_i|H_{ai} \simeq N(\pm \lambda_i^{1/2},1)$, with noncentrality parameter

$$\lambda_i = [1 - \sigma^2_{\hat{y}i} / \sigma^2_{y_i}][\nabla_i / \sigma_{y_i}]^2 \ , \tag{15}$$

in which ∇_i is the postulated model error in the i^{th} observable, and $\sigma^2_{\hat{y}i}, \sigma^2_{yi}$ are the a-posteriori and a-priori variances of the i^{th} observable respectively. The identification step now consists of comparing for i=1,..,m, at the levels of significance α_i, the sample values of the $|\underline{w}_i|$ with the critical values $N_{0.5\alpha i}(0,1)$ of the standard normal distribution. Observations for which the sample value of the $|\underline{w}_i|$ exceed the corresponding critical value are then considered to be identified as outlying observations. This concludes the identification step. After identification of the most likely model error(s), adaptation of the navigation solution is needed so as to eliminate the presence of biases. For the above model this is accomplished by simply omitting the identified observations from the navigation solution.

4.4. Reliability

In the previous section the teststatistics for detection and identification were given. The performance of these teststatistics however, still remains to be discussed. A very important concept in statistical testing is the power of a test. It is the probability of rejecting the null-hypothesis when the alternative hypothesis is indeed true. The power γ of a statistical test depends on the chosen level of significance α, the number of degrees of freedom b and the noncentrality parameter λ. In symbolic notation: $\gamma=\gamma(\alpha,b,\lambda)$. The power is a monotonic increasing function in α and λ, and a monotonic decreasing function in b. Since the noncentrality parameter λ depends on the assumed model errors in H_o, the power function can be used to determine how well particular model errors can be detected or identified with the associated test. Hence, it enables us to answer important questions as: 'What size of model error should the i^{th} observable at least have, in order for it to be detected or identified with at least a probability γ at a fixed level of significance α?' (internal reliability), and 'How do model errors in the observables manifest themselves as biases in the navigation solution?' (external reliability). Navigation applications of the theory of reliability are treated in [32,33,39,40].

Internal reliability:

In order to determine the size of the model errors that can be detected or identified, we make use of the *inverted* power function: $\lambda=\lambda(\alpha,b,\gamma)$. With the inverted power function and expression (15) for the noncentrality parameter, we obtain the following expression for the sizes of the one-dimensional model errors:

$$(16) \qquad |\nabla_i| = \sigma_{y_i} \left(\frac{\lambda(\alpha=\alpha_i, b=1, \gamma=\gamma_o)}{[1 - \sigma^2_{\hat{y}_i}/\sigma^2_{y_i}]} \right)^{1/2} \quad \text{for } i=1,..,m \ .$$

The scalar $|\nabla_i|$ determines the size of the model error the i^{th} observation should have at least, in order that it be identified with a probability γ_o at the level of significance α_i by the w_i-test. The scalar $|\nabla_i|$ is called the *minimal detectable bias* (MDB) of the i^{th} observable. The set of MDB's for i=1,..,m, is said to describe the *internal* reliability of the model. The internal reliability is poor if the MDB's are too large, and the internal reliability is good if the MDB's are small enough. Note that the internal reliability is infinitely poor in case $\sigma^2_{\hat{y}i} = \sigma^2_{yi}$. In this case any error in the i^{th} observable will pass the test unnoticed. It follows from (16) that the MDB's depend on:

i) the chosen level of significance α_i and power γ_o,
ii) the a-priori precision σ^2_{yi} of the pseudo ranges, and
iii) the receiver-satellite geometry through the design matrix **A**.

As an example of how the receiver-satellite geometry effects the internal reliability of a redundant GPS single point positioning fix, table 4 shows the MDB's of a fix taken in Delft on 29-10-90 at 21 hr. The redundancy equalled b=m-4=2, and the level of significance and power were set at α=0.001 and γ=0.80 respectively, giving a noncentrality parameter of λ=17.075. The average horizontal precision in terms of the horizontal delution of precision was good, HDOP=1.23. The results of table 4 show however that a sufficient precision in the navigation solution need not necessarily correspond with a sufficient internal reliability. The quality of a navigation solution should therefore always be judged on both precision *and* reliability.

When the skyplot of figure 16 is compared with table 4, the following remarks can be made. First note that satellites 1 and 5 are close together. The two pseudo ranges to satellites 1 and 5 therefore check each other well. This explains the relatively small and almost equal MDB's for the first and fifth pseudo range. Also note that in the absence of satellite 3, one would expect, due to symmetry, the MDB's of pseudo range 2 and 6 to be of the same order. With satellite 3 however, additional redundancy for checking pseudo range 2 enters, which explains why its MDB is smaller than that of pseudo range 6.

Finally note the high value for the MDB of the fourth pseudo range. This is due to the fact that the line-of-sight vector to satellite 4 is not too far from the symmetry axis of the remaining line-of-sight vectors. See also [41]. In other words, without pseudo range 4 the precision in the direction of the fourth satellite would be rather poor.

Satellite No.	$\lvert\nabla\rvert/\sigma$
1 PRN 16	5.41
2 PRN 18	8.81
3 PRN 2	5.25
4 PRN 9	69.55
5 PRN 6	5.62
6 PRN 17	22.63

Table 4: GPS internal reliability

```
85-90N----------------E----------------S----------------W----------------N
80-85|                                                                   |
75-80|                                                                   |
70-75|                                                                   |
65-70|                                        5                          |
60-65|                                        1                          |
55-60|                                                                   |
50-55|                                                                   |
45-50|                                                                   |
40-45|                       3                                           |
35-40|                                                                   |
30-35|                                                                   |
25-30|                                                                   |
20-25|                                                                   |
15-20|                  2                     4                  6       |
10-15|                                                                   |
 5-10|                                                                   |
 0- 5N----------------E----------------S----------------W----------------N
```

Figure 16: GPS Skyplot, elevation versus azimuth.

External reliability:

In order to be able to judge the relevance of internal reliability, it is of importance to know how the model errors manifest themselves as biases in the estimator $\hat{\underline{x}}$ or functions thereof. For instance, a large MDB need not necessarily propagate as a large bias into the parameters of interest. When one considers the impact of model errors, one should make clear on what functions of $\hat{\underline{x}}$ the impact is studied. This depends very much on the particular application for which the navigation system is designed. For instance, the impact on instrumental parameters may or may not be of interest, or one may particularly be interested in velocity but not in position, or, as is the case in some GPS-applications, it is the horizontal solution which is of interest and not the individual pseudo range bias. In all these cases one generally has a set of linear(ized) functions of $\hat{\underline{\mathbf{x}}}$ that is of particular interest. If we collect these functions in a matrix $\mathbf{F}^*$, then it is the bias $\nabla\hat{\mathbf{f}}$ in $\hat{\underline{\mathbf{f}}}=\mathbf{F}^*\hat{\underline{\mathbf{x}}}$ that is of interest. Using (14), these biases may be computed for every MDB as:

$$\nabla_i\hat{\mathbf{f}} = \mathbf{F}^*Q_{\hat{\mathbf{x}}}\,\mathbf{A}^*Q^{-1}\mathbf{c}_i|\nabla_i| \;,$$

with $\mathbf{c}_i$ the canonical unit vector with a 1 in the i^{th}-place. For i=1,..,m, this set is said to describe the *external* reliability of the model.

In table 5 we have given the with table 4 and figure 16 corresponding external reliability. Note the large impact on position of the MDB of the fourth pseudo range. Also note that the MDB of the sixth pseudo range mainly affects the north component of position. Compare this with the skyplot of figure 16.

Satellite No.	$\nabla x/\sigma$ (East)	$\nabla y/\sigma$ (North)	$\nabla z/\sigma$ (Up)
1 PRN 16	0.50	-0.19	-3.76
2 PRN 18	-4.13	-0.11	4.60
3 PRN 2	-1.41	0.52	-1.25
4 PRN 9	32.37	50.09	65.67
5 PRN 6	0.26	-0.57	-4.50
6 PRN 17	2.99	-15.14	6.01

Table 5: GPS external reliability

An application:

Let us now, in order to illustrate how the theory can be applied, consider the use of GPS for civil aviation. The GPS position performance requirements which have been developed by the U.S. Radio Technical Commission for Aeronautics (RTCA) are presented in table 6 [42].

The *maximum allowable alarm rate* of the table refers to the total average alarm rate with the equipment in normal operation with no satellite malfunction. And *time to alarm* is defined to be the maximum allowable elapsed time from the onset of a GPS-failure until the time that the alarm is annunciated. The 'maximum allowable alarm rate' together with 'time to alarm' therefore determine the acceptable level of significance α. For the en route phase a maximum allowable alarm rate of 0.0002/hr with a decision every 30 sec gives a level of significance of $\alpha = 0.0002 \times 30/3600 = 1.7 \times 10^{-6}$.

Phase of flight	Maximum Allowable Alarm Rate	Time to Alarm	Minimum Detection Probability	Alarm Limit
En route	0.0002/Hr	30 sec	0.999	3667 mtr (2.0 nmi)
Terminal	0.0002/Hr	10 sec	0.999	1833 mtr (1.0 nmi)
Approach (non-precision)	0.0002/Hr	10 sec	0.999	550 mtr (0.3 nmi)

Table 6: GPS position performance requirements

The *minimum detection probability* equals the required power γ and is specified for single satellite failures. The minimum power for the conventional alternative hypotheses is thus specified at the level of γ_o=.999. Finally, the *alarm limit* of table 6 implies that a GPS-failure is defined to exist when the external reliability in terms of the navigation horizontal radial bias is greater than the stated alarm limit. Thus with $\nabla_i\hat{\mathbf{f}}=(\nabla_i\hat{x},\nabla_i\hat{y})^*$, the requirement for the external reliability reads for the en route phase: $\|\nabla_i\hat{\mathbf{f}}\| = \{(\nabla_i\hat{x})^2 + (\nabla_i\hat{y})^2\}^{1/2} \leq 2.0$ nmi, for $i=1,..,m$.
With the above requirements it is now possible to initialize the quality control process. Since identification of outlying pseudo ranges is not required in the above RTCA-specifications, the monitoring is restricted to detection only. For the en route phase, detection proceeds then as follows:

i) A GPS-failure is declared to have occurred if

$$T = \hat{\mathbf{e}}^*\mathbf{Q}^{-1}\hat{\mathbf{e}} > \chi^2_\alpha(m-4,0) \;, \text{ with } \alpha=1.7\text{x}10^{-6}.$$

ii) The detection test is declared unreliable if

$$\max_i \|\nabla_i\hat{\mathbf{f}}\| > 2.0 \text{ nmi} \;, \text{ with } \gamma_o=.999 \;.$$

In both cases warnings are provided, stating that the GPS-system should not be used for navigation.

5. REFERENCES

[1] Greenspan, R.L. and J.I. Donna (1986): Measurement Errors in GPS Observables. Proceedings of the Forty-Second Annual Meeting of The Institute of Navigation, Seattle, WA.

[2] Klobuchar, J.A. (1986): Design and Characteristics of the GPS Ionospheric Time Delay Algorithm for Single Frequency Users. PLANS Proceedings, The Institute of Electrical and Electronics Engineers, Inc., New York.

[3] Jorgensen, P.S. (1988): An Assessment of Ionospheric Effects on the GPS User. Navigation, Journal of the Institute of Navigation, Vol. 36, No. 2, pp. 195-204.

[4] Tranquilla, J.M. and J.P. Carr (1991): GPS Multipath Field Observations at Land and Water Sites. NAVIGATION: Journal of The Institute of Navigation, Vol. 37, No. 4.

[5] Bock, Y., R.I. Abbot, C.C. Counselman, S.A. Gourevitch, and R.W. King (1985): Establishment of Three-Dimensional Geodetic Control by Interferometry with the Global Positioning System. Journal of Geophysical Research, 90(B9), pp. 7689-7703.

[6] Goad, C.C. (1986): Precise Positioning with the Global Positioning System. Proceedings Third International Symposium on Inertial Technology for Surveying and Geodesy. Calgary, Canada.

[7] King, R.W., E.G. Masters, C. Rizos, C. Stolz, and J. Collins (1985): Surveying with GPS. Monograph 9. School of Surveying, University of New South Wales, Australia.

[8] Mader, G.L. (1986): Dynamic Positioning Using GPS Carrier Phase Measurements. Manuscripta Geodaetica, 11(4), pp. 272-277.

[9] Remondi, B.W. (1985): Performing Centimeter-Level Surveys in Seconds with GPS Carrier Phases: Initial Results. NOAA Technical Memorandum NOS NGS-43.

[10] Munck, J.C. de (1991): Tropospheric Effects on Baseline Measurements by Using (GPS) Satellites, Report no. 91.3 Department of Geodesy, Fac. of Math. and Phys. Geodesy, TU Delft.

[11] Jong, C.D. de (1991): GPS-Satellite Orbits and Atmospheric Effects, Report no. 91.1 Department of Geodesy, Fac. of Math. and Phys. Geodesy, TU Delft.

[12] Hofmann-Wellenhof, B. and B.W. Remondi (1988): The Antenna Exchange: One Aspect of High-Precision GPS Kinematic Survey, presented at the

international GPS-Workshop, Darmstadt, April 10-13.

[13] Remondi, B.W. (1990): Applying Kinematic GPS Techniques at our Nation's Airports. Proceedings PLANS Symposium, IEEE, pp. 262-266.

[14] Schwarz, K.P., M.E. Cannon, and R.V.C. Wong (1989): A comparision of GPS kinematic models for the determination of position and velocity along a trajectory. Manuscripta Geodaetica, Vol. 14, No. 5, pp. 345-353.

[15] Twembeke, U. van, A. Muls, G.W. Hein, H. Landau, G. Baustert, and K. Hehl (1989): Precise Differential Kinematic Positioning for Hydrographic Surveying Tasks. Marine Geodesy, pp. 253-276.

[16] Loomis, P.V.W. (1989): A Kinematic GPS Double Differencing Algorithm. Proceedings of the Fifth International Geodetic Symposium on Satellite Positioning, New Mexico State University, Las Cruces.

[17] Hatch, R. (1989): Ambiguity Resolution in the Fast Lane. Proceedings of ION GPS-89, pp. 45-50.

[18] Hatch, R. (1990): Instantaneous A,biguity Resolution. Proceedings of Kinematic Systems in Geodesy, Surveying, and Remote Sensing, IAG 107, Springer Verlag, pp. 299-308.

[19] Stancell, T.A. (1986): RTCM SC-104 Recommended Pseudolite Signal Specification. Global Positioning System, Vol. III, The Institute of Navigation, pp. 117-134.

[20] Kalafus, R., A.J. van Dierendonck, and N.A. Pealer (1986): Special Committee 104 Recommendations for Differential GPS Service. Global Positioning System, Vol. III, The Institute of Navigation, 1986, pp. 101-116.

[21] Kremer, G.T., R.M. Kalafus, P.V.M. Loomis, and J.C. Reynolds (1990): The Effect of Selective Availability on Differential GPS Corrections. NAVIGATION, Journal of The Institute of Navigation, Vol. 37, No. 1, pp. 39-52.

[22] RTCM Special Committee No. 104 (1990): RTCM Recommended Standards for Differential NAVSTAR GPS Service.

[23] Teunissen, P.J.G. (1991): De Geodetische Lijn, De Ingenieur, Vol. 103, no. 6/7, pp. 24-30.

[24] Teunissen, P.J.G. (1985): Quality Control in Geodetic Networks. In: Optimization and Design of Geodetic Networks, Springer Verlag, pp. 526-547.

[25] Mierlo, J. van (1975): Statistical Analysis of Geodetic Networks Designed for the Detection of Crustal Movements. In: Progress in Geophysics, Borrodaile G.J. et al. (Eds.). North-Holland Publishing

Company, pp. 45-51.

[26] Kok, J.J. (1982): Statistical Analysis of Deformation Problems Using Baarda's Testing Procedure. In: Forty Years of Thought, Delft, Vol. 2, pp. 470-488.

[27] Staff of LGR (1982): The Delft Approach of the Design and Computation of Geodetic Networks. In: Forty Years of Thought, Delft, pp. 202-274.

[28] Förstner, W. (1982): Results of Test I on Gross Error Detection of ISP WG III/I and OEEPE. ISP Commission III, Helsinki.

[29] Teunissen, P.J.G. (1986): Adjusting and Testing with the Models of the Affine and Similarity Transformation. Manuscripta Geodaetica, Vol. 11, pp. 214-225.

[30] Teunissen, P.J.G. and M.A. Salzmann (1988): Performance Analysis of Kalman Filters. Proceedings of HYDRO 88. Special Publications. No. 23, Hydrographic Society, pp. 185-193.

[31] Teunissen P.J.G. and M.A. Salzmann (1989): A Recursive Slippage Test for Use in State-Space Filtering. Manuscripta Geodaetica, Vol. 14, No. 6, pp. 383-390.

[32] Teunissen P.J.G. (1990): Quality Control in Integrated Navigation Systems. IEEE Aerospace and Electronic Systems Magazine, Vol. 5, No.7, pp. 35-41.

[33] Teunissen P.J.G. (1990): An Integrity and Quality Control Procedure for Use in Multi Sensor Integration. Proceedings of ION-90, pp. 513-522.

[34] Marel, H. v.d. and A. Kösters (1989): Statistical Testing and Quality Analysis of 3-D Networks. Part II: Applications to GPS. IAG Symposium, Edinburgh, pp. 290-297.

[35] Brown, A. (1988): Civil Aviation Integrity Requirements for the Global Positioning System, NAVIGATION, Journal of The Institute of Navigation. Vol. 35, No. 1, pp. 23-39.

[36] Kalafus, R.M. (1989): GPS Integrity Channel RTCA Working Group Recommendations. NAVIGATION, Journal of The Institute of Navigation, Vol. 36, No. 1, pp. 25-44.

[37] Brown, A. (1989): A Multi-Sensor Approach to Assuring GPS Integrity. Presented at RTCA 1989 Technical Symposium.

[38] Teunissen, P.J.G. (1990): Some Aspects of Real-Time Model Validation Techniques for Use in Integrated Systems. Proceedings of Kinematic Systems in Geodesy, Surveying, and Remote Sensing, IAG 107, Springer Verlag, pp. 191-200.

[39] Salzmann, M. (1990): MDB: A Design Tool for Integrated Navigation

Systems. Proceedings of Kinematic Systems in Geodesy, Surveying, and Remote Sensing, IAG 107, Springer Verlag, pp. 218-227.

[40] Lu, G. and G. Lachapelle (1990): Reliability Analysis applied to Kinematic GPS Position and Velocity Estimation. Proceedings of Kinematic Systems in Geodesy, Surveying, and Remote Sensing, IAG 107, Springer Verlag, pp. 273-284.

[41] Teunissen, P.J.G. (1990): GPS op afstand bekeken. In: Snellius Anniversary Volume 1985-1990, pp. 215-233.

[42] RTCA (1991): Minimal Operational Performance Standards for Airborne Supplemental Navigation Equipment using GPS (draft).